AD-A090 625 LEHIGH UNIV BETHLEHEM PA INST OF FRACTURE AND SOLID --ETC F/G 20/11
TRANSIENT HYDROTHERMAL AND MECHANICAL STRESS INTENSITIES AROUND--ETC(U)
AUG 80 G C SIH, A OGAWA DAAG46-79-C-0049

UNCLASSIFIED AMMRC-TR-80-42 NL

1 OF 1
AD A
090625

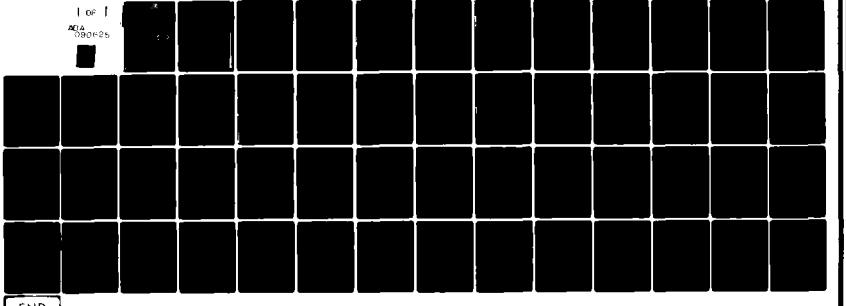

END
DATE FILMED
11-80
DTIC

AD A090625

(1) LEVEL II

AD

AMMRC TR 80-42

TRANSIENT HYGROTHERMAL AND MECHANICAL STRESS INTENSITIES AROUND ELLIPTICAL CAVITIES

August 1980

DTIC
ELECTE
S OCT 2 1 1980 D
B

G. C. Sih and A. Ogawa

Lehigh University
Bethlehem, Pennsylvania 18015

Final Report

Contract Number DAAG46-79-C-0049

Approved for public release; distribution unlimited.

Prepared for

ARMY MATERIALS AND MECHANICS RESEARCH CENTER
Watertown, Massachusetts 02172

DDC FILE COPY

80 10 14 104

The findings in this report are not to be construed as an official Department of the Army position, unless so designated by other authorized documents.

Mention of any trade names or manufacturers in this report shall not be construed as advertising nor as an official indorsement or approval of such products or companies by the United States Government.

DISPOSITION INSTRUCTIONS

Destroy this report when it is no longer needed.
Do not return it to the originator.

Unclassified

SECURITY CLASSIFICATION OF THIS PAGE (When Data Entered)

REPORT DOCUMENTATION PAGE	READ INSTRUCTIONS BEFORE COMPLETING FORM
1. REPORT NUMBER: AMMRC TR-80-42	2. GOVT ACCESSION NO.: AD-A090 625
3. RECIPIENT'S CATALOG NUMBER	
4. TITLE (and Subtitle): TRANSIENT HYGROTHERMAL AND MECHANICAL STRESS INTENSITIES AROUND ELLIPTICAL CAVITIES	5. TYPE OF REPORT & PERIOD COVERED: Final Report
	6. PERFORMING ORG. REPORT NUMBER
7. AUTHOR(s): G. C. Sih and A. Ogawa	8. CONTRACT OR GRANT NUMBER(s): DAAG46-79-C-0049
9. PERFORMING ORGANIZATION NAME AND ADDRESS: Institute of Fracture and Solid Mechanics, Lehigh University, Bethlehem, Pennsylvania 18015	10. PROGRAM ELEMENT, PROJECT, TASK AREA & WORK UNIT NUMBERS: D/A Proj: 1L162105AH84, AMCMS Code: 633304.21500.03
11. CONTROLLING OFFICE NAME AND ADDRESS: Army Materials and Mechanics Research Center, Watertown, Massachusetts 02172	12. REPORT DATE: August 1980
	13. NUMBER OF PAGES: 54
14. MONITORING AGENCY NAME & ADDRESS (if different from Controlling Office)	15. SECURITY CLASS. (of this report): Unclassified
	15a. DECLASSIFICATION/DOWNGRADING SCHEDULE

16. DISTRIBUTION STATEMENT (of this Report)

Approved for public release; distribution unlimited.

17. DISTRIBUTION STATEMENT (of the abstract entered in Block 20, if different from Report)

18. SUPPLEMENTARY NOTES

19. KEY WORDS (Continue on reverse side if necessary and identify by block number)

Hygrothermal effect	Transient response
Moisture content	Composite
Temperature	Crack
Finite element	Stress intensities

20. ABSTRACT (Continue on reverse side if necessary and identify by block number)

The transient hygrothermal stresses are determined by assuming that heat and moisture are coupled. A system of coupled diffusion equations is solved by a finite element scheme allowing for time-dependent changes in the moisture and/or temperature on the surfaces of the T300/5208 epoxy resin for the graphite/epoxy fiber-reinforced composite. The time dependent portion of the problem was solved by means of Laplace transformation. Particular emphases are given to the evaluation of transient stresses around a mechanical

DD FORM 1 JAN 73 1473 EDITION OF 1 NOV 65 IS OBSOLETE

Unclassified

SECURITY CLASSIFICATION OF THIS PAGE (When Data Entered)

imperfection in the form of a narrow ellipse. Numerical results are displayed graphically for three different values of the semi-minor to semi-major axis ratio.

A stress intensity factor parameter commonly used in fracture mechanics is defined for a narrow ellipse and calculated to investigate the influence of stresses induced by hygrothermal and mechanical disturbances. The radius of curvature of the elliptical cavity can significantly affect the combined stress intensity near the cavity ends. The maximum stress intensities occur at different times depending on the cavity geometry and proportion of the hygrothermal and mechanical loading. These results could shed light on composite failure under conditions where heat and moisture play a role.

Foreword

This research work was performed for the Army Materials and Mechanics Research Center at Watertown, Massachusetts under Contract No. DAAG46-79-C-0049 with the Institute of Fracture and Solid Mechanics, Lehigh University, Bethlehem, Pennsylvania. Mr. J. F. Dignam of the AMMRC was project manager and Dr. S. C. Chou as technical monitor. The support and encouragement of Mr. Dignam and Dr. Chou are gratefully acknowledged.

Accession For
NTIS GRA&I ☑
DTIC TAB ☐
Unannounced ☐
Justification
By
Distribution/
Availability Codes
Dist | Avail and/or Special
A

TRANSIENT HYGROTHERMAL AND MECHANICAL STRESS INTENSITIES AROUND ELLIPTICAL CAVITIES

by

G. C. Sih
Institute of Fracture and Solid Mechanics
Lehigh University
Bethlehem, Pennsylvania 18015 USA

and

Akinori Ogawa*
National Aerospace Laboratory
Tokyo, Japan

ABSTRACT

The transient hygrothermal stresses are determined by assuming that heat and moisture are coupled. A system of coupled diffusion equations is solved by a finite element scheme allowing for time-dependent changes in the moisture and/or temperature on the surfaces of the T300/5208 epoxy resin for the graphite/epoxy fiber-reinforced composite. The time dependent portion of the problem was solved by means of Laplace transformation. Particular emphases are given to the evaluation of transient stresses around a mechanical imperfection in the form of a narrow ellipse. Numerical results are displayed graphically for three different values of the semi-minor to semi-major axis ratio.

A stress intensity factor parameter commonly used in fracture mechanics is defined for a narrow ellipse and calculated to investigate the influence of stresses induced by hygrothermal and mechanical disturbances. The radius of curvature of the elliptical cavity can significantly affect the combined stress in-

*This work was completed in the U.S. when Akinori Ogawa held the position of Visiting Scientist at the Institute of Fracture and Solid Mechanics at Lehigh University.

tensity near the cavity ends. The maximum stress intensities occur at different times depending on the cavity geometry and proportion of the hygrothermal and mechanical loading. These results could shed light on composite failure under conditions where heat and moisture play a role.

INTRODUCTION

One of the main concerns of using advanced fiber-reinforced polymeric matrix composites as aerospace structural components is the degradation of the material due to moisture at elevated temperatures. This is of particular concern to the matrix-dominated composite. The deterioration of material properties cannot be easily understood without a sound analytical modeling of the physical problem. A majority of the present workers in this field [1-3] assume that temperature and moisture do not interact and that they each obey the simple (Fickian) diffusion theory. As a consequence, experimental data are available only for changes in the moisture condition [4] while the temperature environment is taken to be constant. In contrast to the common belief, coupling between temperature and moisture can be extremely important [5,6] when the surface temperature undergoes rapid changes. The difference in the hygrothermal stresses with and without coupling can differ anywhere from 20 to 80% depending on the surface temperature gradient. This casts a new light on the subject and suggests a series of new experiments before reliable predictions on the life of structural components due to service environments could be made.

In two recent publications, the transient hygrothermal stresses around a spherical [7] and circular [8] cavity were determined. The stresses were found to oscillate in time and vary in a complicated nature depending on the boundary condition whether moisture and/or temperature are applied to the cavity. An

analysis was also performed in [8] to investigate the possible sites of failure. The hygrothermally and mechanically induced stresses were found to peak at distances away and near the cavity, respectively. Based on the minimum strain energy density criterion, actual locations of possible failure were determined and discussed in detail.

The primary objective of this investigation is to develop an analytical method for determining the redistribution of hygrothermal and mechanical stresses due to narrow elliptically-liked defects such that the initiation of failure in composites exposed to service environments could be better understood. Use is made of the time-dependent finite element method developed in an earlier publication [8]. Different grid patterns are constructed as the aspect ratios of the elliptical flaw are altered. Presented graphically are hygrothermal stresses near the ellipse for different time from which time dependent stress intensity factors can be defined to study the resistance of the T300/5208 epoxy resin to fracture.

MATHEMATICAL MODEL

The thermodynamic treatment for deriving the coupled diffusion equations is given in [9] and will not be repeated here. If T stands for the temperature and C the mass of moisture per unit volume of void space in the solid, then the governing equations take the forms

$$D\nabla^2 C - \frac{\partial}{\partial t}(C - \lambda T) = 0$$

$$D\nabla^2 T - \frac{\partial}{\partial t}(T - \nu C) = 0 \qquad (1)$$

in which D and $\mathcal{D}$ are the diffusion coefficients with units of area per unit time and λ and ν are the coupling coefficients with units of mass per unit volume per unit temperature and the reciprocal, respectively. The Laplace operator in equations (1) is in two dimensions given by $\nabla^2 = \partial^2/\partial x^2 + \partial^2/\partial y^2$. The domain of interest is that of a multiply-connected rectangular region R having the dimensions: 6 units in height and 8 units in width. A narrow elliptical opening with semi-major axis a of one unit and variable semi-major axis b is centered at the origin of a rectangular coordinate system (x,y) and is shown in Figure 1. Initially for t<0, the region R possesses the following temperature and moisture fields:

$$T(x,y,t) = T_o(x,y)$$
$$C(x,y,t) = C_o(x,y) \qquad (2)$$

For t>0, the temperature and/or moisture on the boundary Γ_I and/or Γ_{II} are changed such that equations (2) become

$$T(x,y,t) = T_o(x,y) + \Delta T(x,y,t)$$
$$C(x,y,t) = C_o(x,y) + \Delta C(x,y,t) \qquad (3)$$

Once the boundary conditions at $t = t_o$ are known, equations (1) may be solved numerically for T(x,y,t) and C(x,y,t).

The time dependent two-dimensional finite element method developed in [8] will be applied to evaluate equations (1). The two types of boundary conditions

are *sudden moisture change* with

$$\Delta C = \begin{cases} 0 & \text{on } \Gamma_I \\ \Delta C_B & \text{on } \Gamma_{II} \end{cases} \qquad (4)$$

$$\Delta T = 0 \text{ on } \Gamma_I \text{ and } \Gamma_{II}$$

and *sudden temperature change* with

$$\Delta C = 0, \text{ on } \Gamma_I \text{ and } \Gamma_{II}$$

$$\Delta T = \begin{cases} 0 & \text{on } \Gamma_I \\ \Delta T_B & \text{on } \Gamma_{II} \end{cases} \qquad (5)$$

Since the problem is one-quarter symmetry, there is only the need to consider the grid pattern shown in Figure 2 consisting of 100 nodal points. The elements near the elliptical cavity are smaller in size so as to accommodate the high gradient of the local moisture and temperature. In fact, special consideration is given to the sub-region A enclosed by the corner nodes 6, 27, 48 and 47. Depending on the ratio of b/a or the radius of curvature defined by $\rho = b^2/a$, special grid patterns are constructed as shown in Figures 3 to 5. Table 1 outlines the three different aspect ratios of the elliptical opening that will be analyzed. The results will be presented subsequently.

NUMERICAL RESULTS ON DIFFUSION

The system of equations (1) is solved numerically by subjecting the elliptical cavity to sudden changes in the surface moisture and/or temperature according

Table 1 - Three different aspect ratios of the elliptical opening with a=1 unit

Figure number	Semi-minor axis b or (b/a)	Radius of curvature
3	0.200	0.0400
4	0.100	0.0100
5	0.067	0.0044

to the conditions described by equations (4) and/or (5). The moisture and temperature distribution are assumed to be constant in the direction normal to the xy-plane. For the T300/5208 epoxy resin material, the coupling constants are [6] given by $D/\mathcal{D} = 0.1$, $\lambda = 0.5$ and $\nu = 0.5$. Of particular interest is the variation of C and T in the material ahead of elliptical cavity as a function of time.

Figures 6 to 12 give the results for the case when the surface moisture on the ellipse is suddenly raised to another constant value, while the surface temperature is unchanged. Refer to the conditions in equations (4). The initial and final condition on the outside boundary of R in Figure 1 are maintained constant at all time. Plots of $(C-C_o)/(C_f-C_o)$ versus x/a for different values of $\mathcal{D}t/a^2$ are shown in Figures 6 to 8 with b/a varying from 0.2 to 0.067. The end point of the narrow ellipse is given by x/a = 1.0. Initially, the moisture drops very rapidly in the vicinity of the elliptical cavity and it gradually diffuses into the material as time is increased. In the absence of mechanical tensile loading, moisture diffusion tends to decrease with decreasing b/a ratio or radius of curvature of the ellipse $\rho = b^2/a$. This can be seen from the curves in Figures 6 to 8 although the differences are not appreciable. The transient behavior of the temperature is exhibited in Figures 9 to 11 as b/a is varied. The quantity $(T-T_o)/\nu(C_f-C_o)$ is seen to peak very sharply at first and the vari-

ations become more gradual as time increases. The peaks move into the material with decreasing amplitude and they take lower values as the ellipse becomes more slender.

The disturbances within the solid due to coupling of heat and moisture are considerably more pronounced when the surface temperature on the elliptical cavity undergoes rapid changes, equations (5). Figures 12 to 14 give the variations of $(T-T_o)/(T_f-T_o)$ with x/a and time. For small time, only the material near the ellipse experiences temperature change. The temperature gradient tends to spread over a larger portion of the material as time goes by. Again, $(T-T_o)/(T_f-T_o)$ increases with the ratio b/a. Numerical results of $(C-C_o)/\lambda(T_f-T_o)$ versus x/a for the case of sudden temperature change are similar to those shown in Figures 9 to 11 except for the factor $\mathcal{D}/D$ which is equal to ten in the present problem, i.e.,

$$\left[\frac{C-C_o}{\lambda(T_f-T_o)}\right]_{\Delta T = \text{const}} = \frac{\mathcal{D}}{D}\left[\frac{T-T_o}{\nu(C_f-C_o)}\right]_{\Delta C = \text{const}} \tag{6}$$

Hence, there is no need to duplicate them separately.

HYGROTHERMAL STRESSES

For an isotropic and homogeneous material, the hygrothermal stresses may be obtained as

$$\sigma_{ij} = E(\varepsilon_{ij} - \alpha\Delta T\delta_{ij} - \beta\Delta C\delta_{ij}) \tag{7}$$

in which E is the Young's modulus, α the coefficient of thermal expansion and β the coefficient of moisture expansion. The stress and strain components are de-

noted respectively by σ_{ij} and ε_{ij}. The condition of plane strain with $\varepsilon_z = 0$ will be assumed such that

$$\sigma_z = \nu_p(\sigma_r+\sigma_\theta) \tag{8}$$

with ν_p being the Poisson's ratio. The material properties pertaining to T300 /5208 are given as follows:

$$\begin{aligned} &\alpha = 4.5 \times 10^{-5} \text{ m/m°C} \\ &\beta = 2.68 \times 10^{-3} \text{ m/m/\% } H_2O \\ &E = 3.45 \text{ GN/m}^2 \ (5 \times 10^5 \text{ psi}) \\ &\nu_p = 0.34 \end{aligned} \tag{9}$$

For clarity sake, the discussion for the cases of moisture change and temperature change will be carried out separately.

Sudden Application of Moisture. When the moisture on the elliptical cavity is suddenly raised, there results a nonuniform expansion and contraction of material which, in turn, give rise to stresses and strains. Figures 15 to 17 show that the radial stresses are compressive along the line of symmetry ahead of the ellipse. They are highly influenced by the radius of curvature of the ellipse. Note from Figures 15 to 17 that σ_r decreases very sharply as b/a is reduced. This drop increases in magnitude with time and gradually diminishes away from the cavity. The results for the circumferential stresses are given in Figures 18 to 20. Unlike σ_r, σ_θ starts out in compression and then becomes tensile for small time. Again, the magnitude of σ_θ is increased greatly for the more slender el-

liptical cavity in Figure 20.

Sudden Application of Temperature. The stresses resulting from a sudden change of the surface temperature in the cavity boundary are qualitatively different from those discussed earlier. The radial stresses in Figures 21 to 23 are no longer always compressive. For $\mathcal{D}t/a^2 = 4.0$, σ_r first becomes tensile rising to a peak and then becomes compressive. This peak increases with decreasing b/a. For small time, σ_r oscillates violently near the cavity end and returns to zero at x/a = 1. Similarly, the circumferential stresses displayed graphically in Figures 24 to 26 are also tensile for $\mathcal{D}t/a^2 = 4.0$ attaining their largest values at x/a = 1.0 and then decrease in magnitude until they become compressive. The opposite trend is observed for small time, i.e., σ_θ is compressive near the cavity and tensile away from the cavity. The transverse normal stress component σ_z may be obtained from equation (8) from the results in Figures 15 to 26 in a straightforward manner and no special treatment is needed.

TIME DEPENDENT STRESS INTENSITY FACTOR

It is well-known that mechanical imperfections can interact with the sudden changes in moisture and/or temperature in the material causing it to degrade in strength and/or fracture toughness. A parameter that has been commonly used in fracture mechanics [10] is the stress intensity factor whose critical value for a given material can be related to the energy required to initiate the propagation of a line crack. If the stresses are symmetric with respect to the crack plane, only a single parameter k_1 is needed to describe the intensity of the local stresses. Since the hygrothermal stress field is time dependent, the resulting stress intensity factor k_1 will also fluctuate with time.

In addition to the hygrothermal stresses, mechanical stresses will also assume to be present owing to a uniform static tensile load σ_0 applied normal to the crack which is approximated by a narrow ellipse with radius of curvature ρ. Since the stresses induced by diffusion are not coupled with the mechanical stresses, the combined k_1 factor may be obtained by superposition:

$$k_1 = \sigma_0\sqrt{a}\ [1 \pm \frac{1}{2}\ (\frac{\sigma_\theta}{\sigma_0})\ \sqrt{\frac{\rho}{a}}] \tag{10}$$

In the absence of heat and moisture, $\sigma_\theta = 0$ and equation (10) reduces to the familiar result of $k_1 = \sigma_0\sqrt{a}$.

Figures 27 to 29 display the variations of the normalized stress intensity factor $k_1/\sigma_0\sqrt{a}$ with time for three different values of the applied mechanical stress σ_0 = 1.0, 0.1 and 0.01 having the units MN/m^2. The temperature on the crack surface is raised suddenly introducing additional stresses. When σ_0 is relatively large, Figure 27 shows that $k_1/\sigma_0\sqrt{a}$ is not sensitive to changes in b/a. All the curves rise slowly to a peak at $\mathcal{D}t/a^2 \simeq 4.5$ and then decrease in magnitude. In the limit as $t\to\infty$, $k_1 = \sigma_0\sqrt{a}$ is recovered. The hygrothermal effect becomes more pronounced when the applied mechanical stress σ_0 is reduced in magnitude, Figure 28. For σ_0 = 0.1 MN/m^2, the maximum value of k_1 = 3.61 $\sigma_0\sqrt{a}$ occurs at b/a = 0.20 and occurs at $\mathcal{D}t/a^2 \simeq 4.5$. The peaks for k_1 decreases as b/a is decreased and occur at a later time. A similar trend is also observed in Figure 29 when σ_0 is further reduced to 0.01 MN/m^2.

Depending on the gradient of the applied moisture and/or temperature, the hygrothermal stresses alone could lead to failure. The additional mechanical stresses can further aggravate the state of affairs near the crack and cause the crack to run. The results presented in Figures 27 to 29 offer some insight into

the fracture toughness requirement for the T300/5208 resin material when both hygrothermal and mechanical disturbances are present.

CONCLUDING REMARKS

The simultaneous diffusion equations for the coupling of heat and moisture have been solved for a region containing a crack-like imperfection. Studied in detail are the influence of the crack tip radius of curvature modeled by a narrow ellipse on the redistribution of the hygrothermal stresses. The stresses near the crack front are found to vary more sharply as the ellipse becomes more slender. Because of the time dependent nature of the diffusion process, the stresses tend to oscillate and can be either compressive or tensile depending on the elapsed time.

The coupling of heat and moisture is particularly significant when the crack boundary temperature is raised suddenly. The maximum intensification of the local stresses occurs at $\mathcal{D}t/a^2 \simeq 4.5$. The crack tip radius of curvature ρ affects the local hygrothermal and mechanical stresses in different ways. The former tends to increase with ρ while the latter behaves in the opposite fashion. It is a combination of loading and geometry that must be analyzed for determining the critical condition of crack instability.

REFERENCES

[1] D. R. Tenney and J. Unnam, "Analytical Prediction of Moisture Absorption in Composites", Journal of Aircraft, Vol. 15, No. 3, pp. 148-154, 1978.

[2] Y. Weitsman, "Diffusion with Time-Varying Diffusivity with Application to Moisture-Sorption in Composites", Journal of Composite Materials, Vol. 10, pp. 193-204, 1976.

[3] H. C. Carter and K. C. Kibler, "Langmuir-Type Model for Anomalous Moisture Diffusion in Composite Resins", Journal of Composite Materials, Vol. pp. 118-131, 1978.

[4] C. H. Shen and G. S. Springer, "Moisture Absorption and Desorption of Composite Materials", Journal of Composite Materials, Vol. 10, pp. 2-20, 1976.

[5] R. J. Hartranft and G. C. Sih, "The Influence of Coupled Diffusion of Heat and Moisture on the State of Stress in a Plate", Journal of Polymer Mechanics, Mekhanika Polimerov, USSR (in press).

[6] G. C. Sih, M. T. Shih and S. C. Chou, "Transient Hygrothermal Stresses in Composites: Coupling of Moisture and Heat with Temperature Varying Diffusivity", International Journal of Engineering Science, Vol. 18, pp. 19-42, 1980.

[7] R. J. Hartranft and G. C. Sih, "Stresses Induced in an Infinite Medium by the Coupled Diffusion of Heat and Moisture from a Spherical Hole", International Journal of Engineering Fracture Mechanics (in press).

[8] G. C. Sih and A. Ogawa, "Two-Dimensional Transient Hygrothermal Stresses in Bodies with Circular Cavities: Moisture and Temperature Coupling Effects", Institute of Fracture and Solid Mechanics Technical Report, Lehigh University, July 1980.

[9] R. J. Hartranft and G. C. Sih, "The Influence of the Soret and DuFour Effects on the Diffusion of Heat and Moisture in Solids", International Journal of Engineering Science (in press).

[10] G. C. Sih and B. Macdonald, "Fracture Mechanics Applied to Engineering Problems - Strain Energy Density Fracture Criterion", Journal of Engineering Fracture Mechanics, Vol. 6, pp. 361-386, 1974.

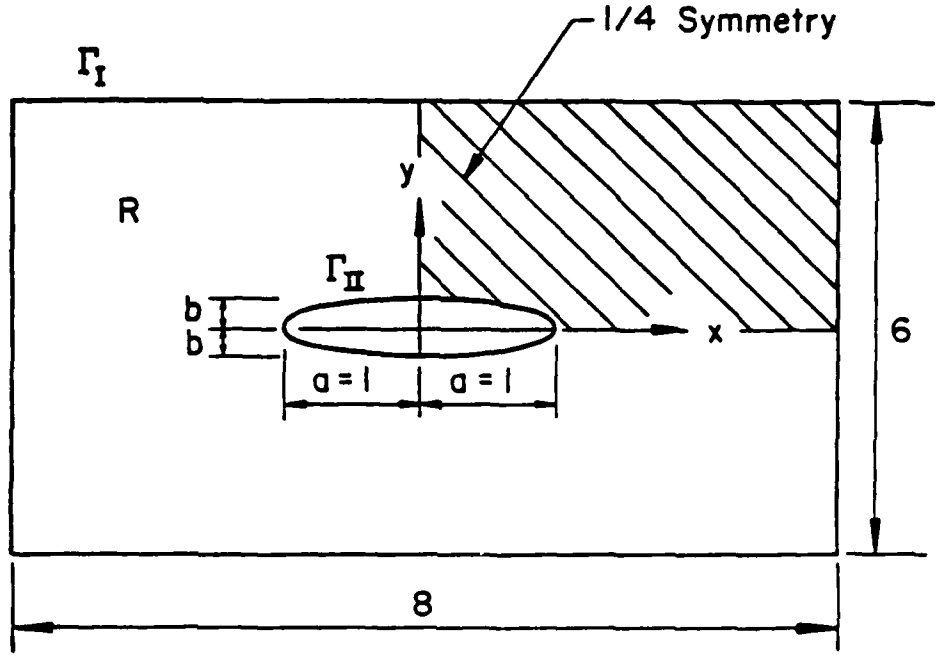

Figure 1 - A rectangular region with an elliptical opening

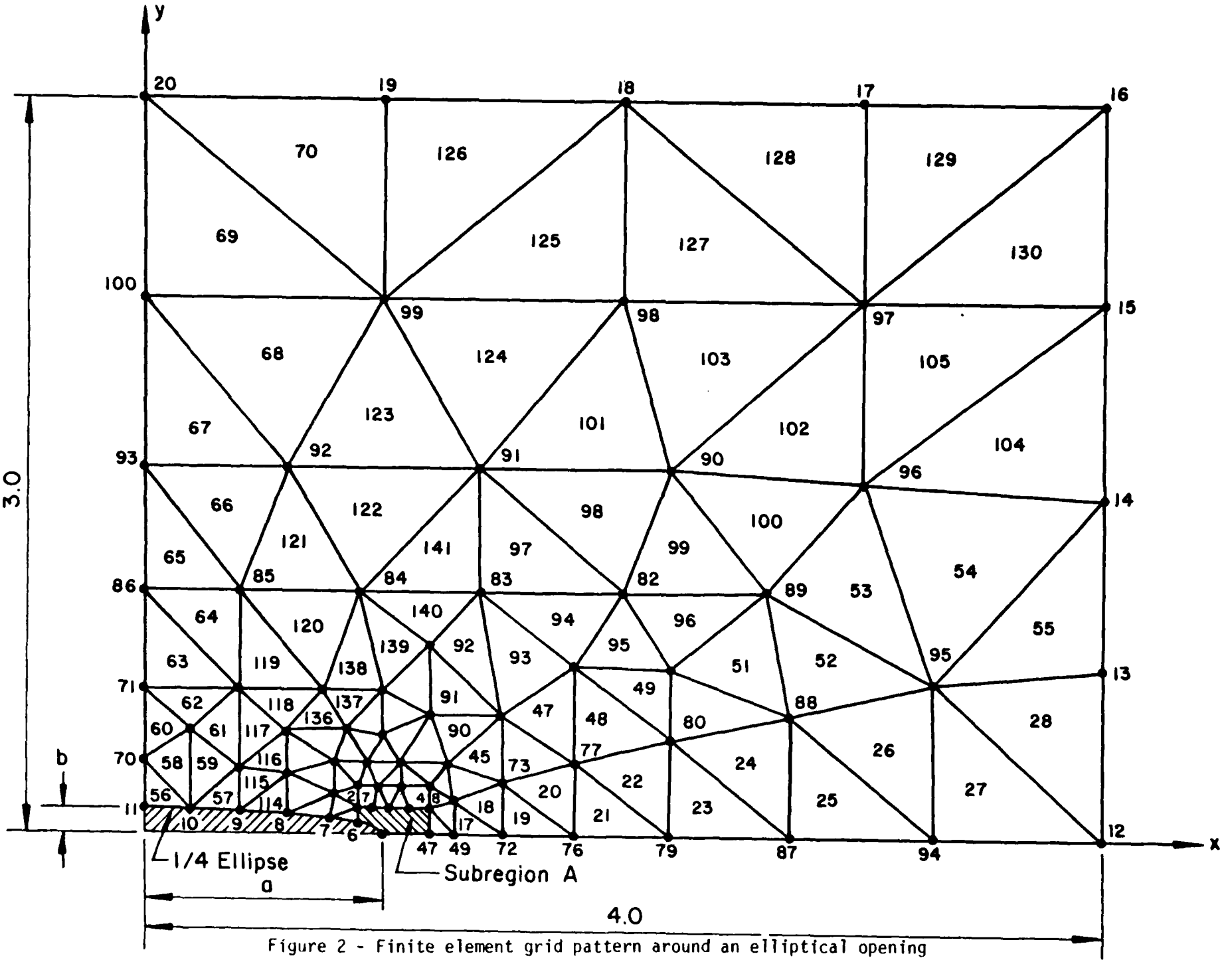

Figure 2 - Finite element grid pattern around an elliptical opening

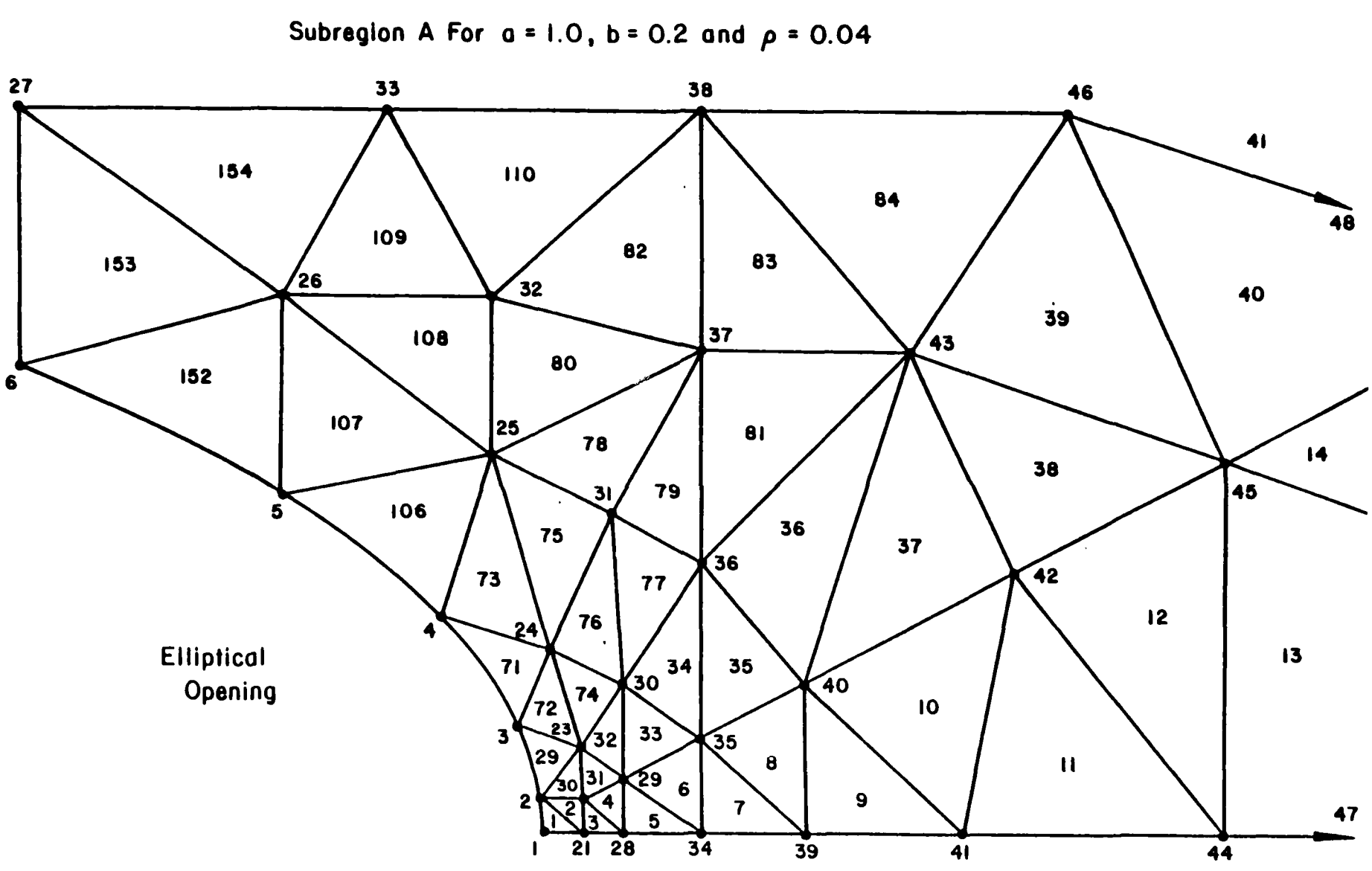

Figure 3 - Subregion ahead of ellipse with b/a = 0.2

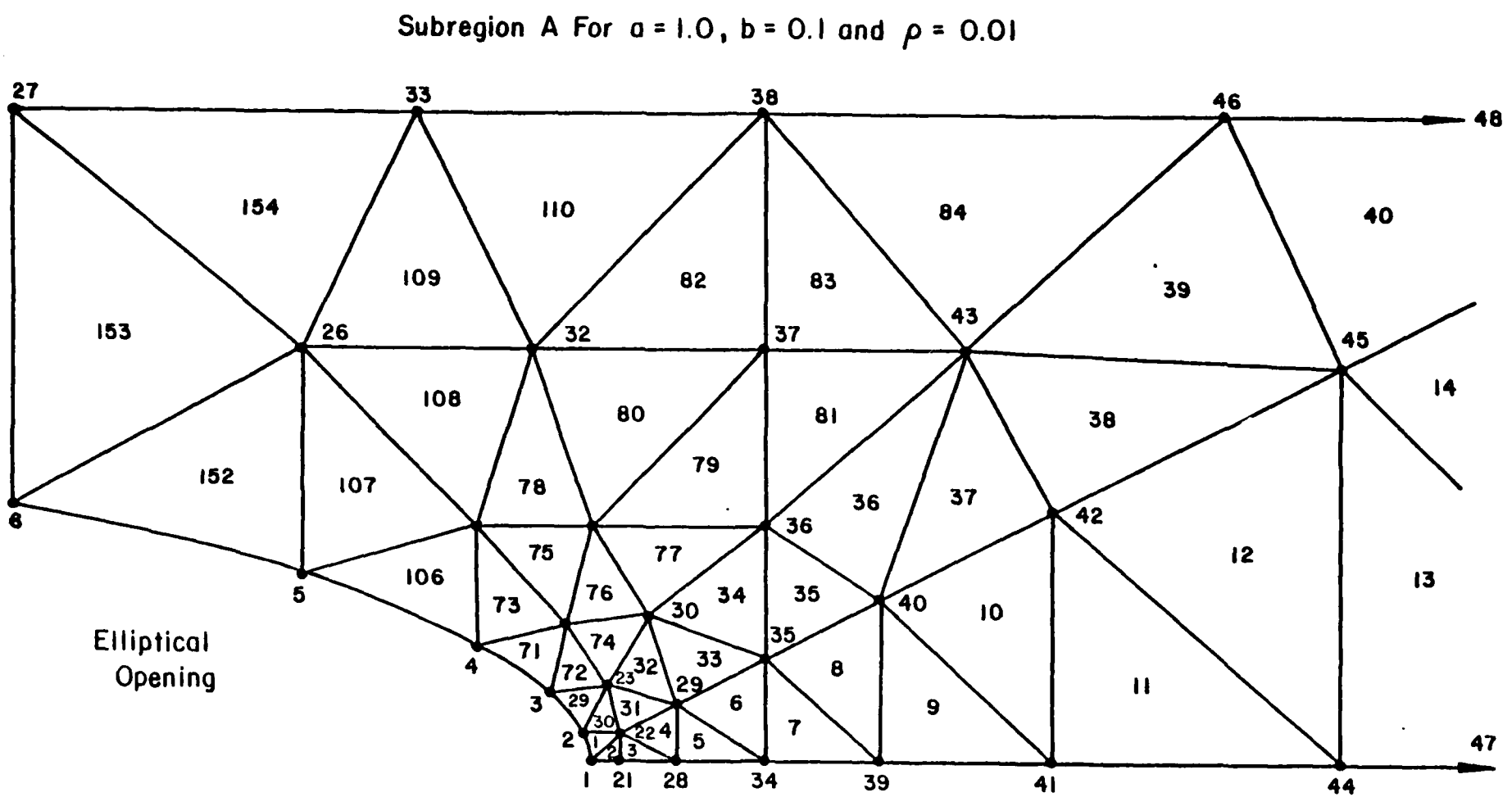

Figure 4 - Subregion ahead of ellipse with b/a = 0.1

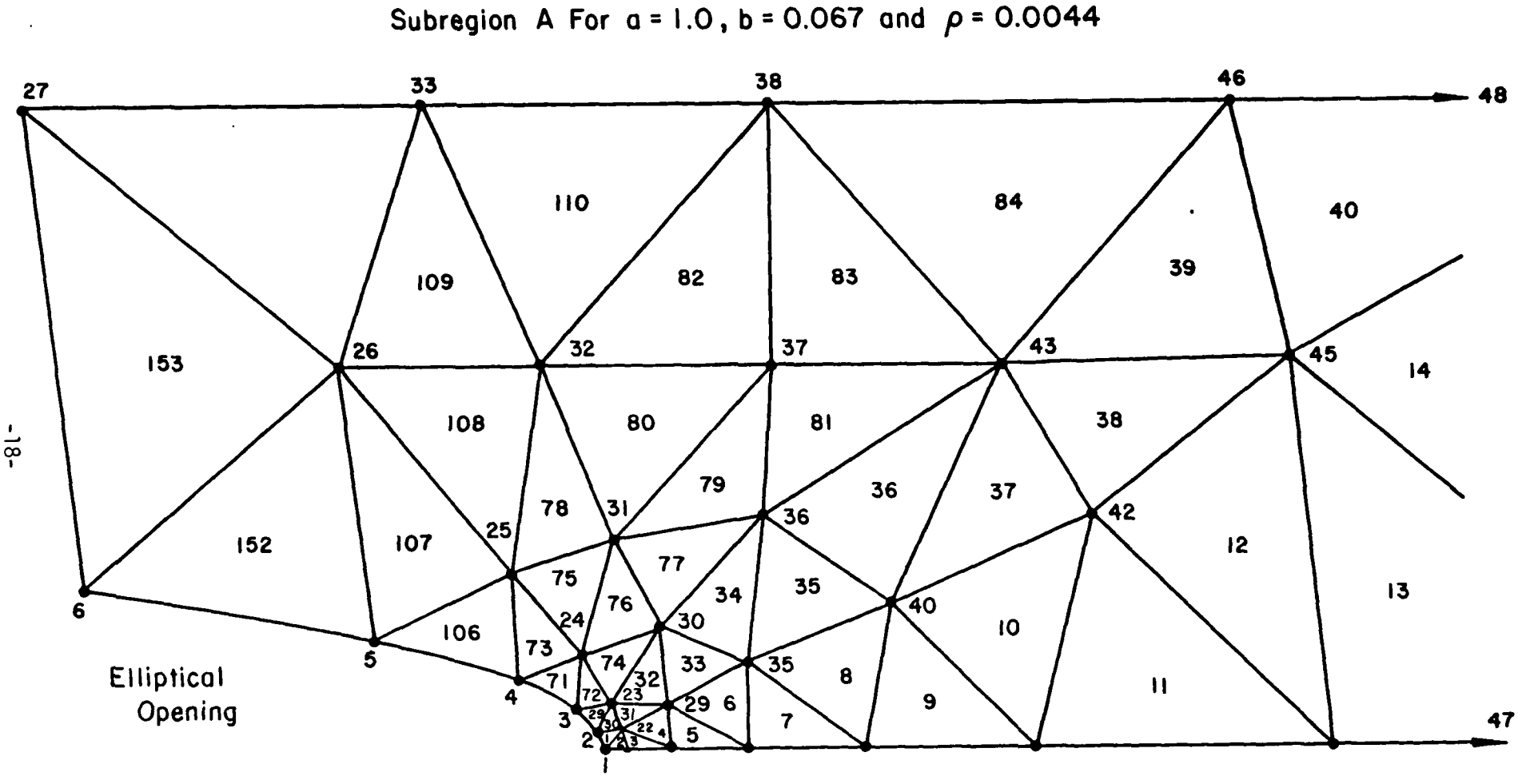

Figure 5 - Subregion ahead of ellipse with b/a = 0.067

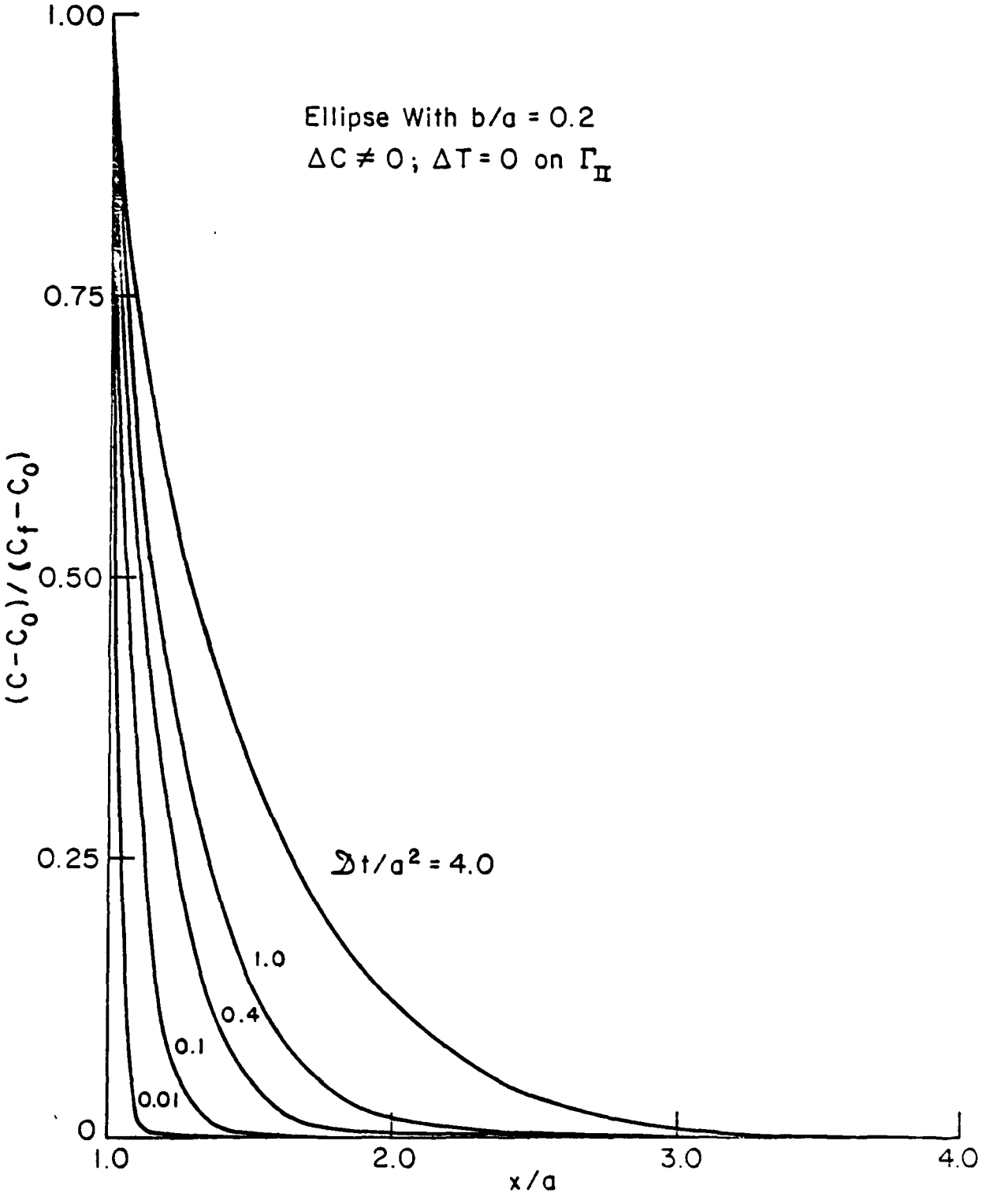

Figure 6 - Normalized moisture content versus distance for b/a = 0.2 and sudden moisture change

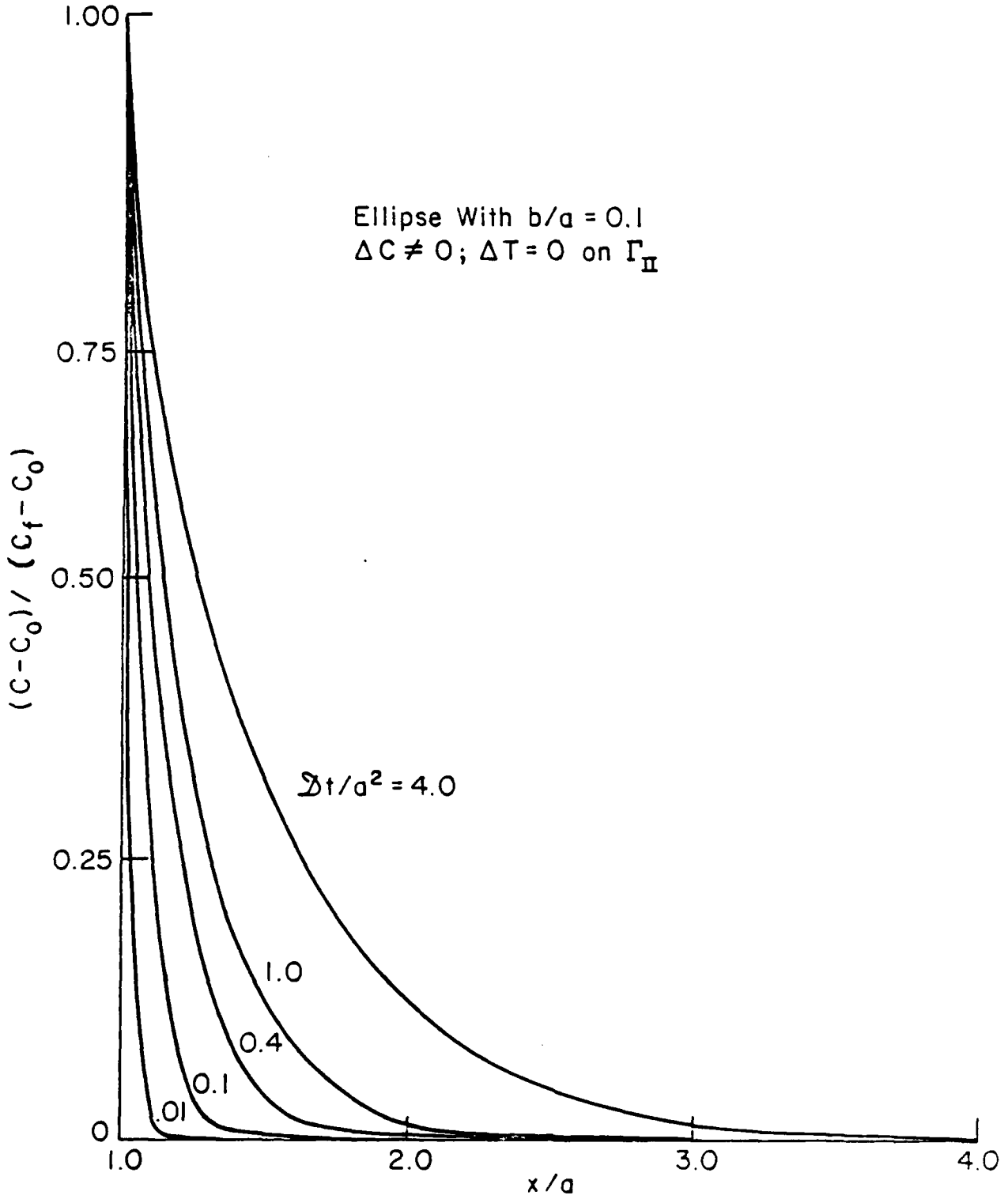

Figure 7 - Normalized moisture content versus distance for b/a = 0.1 and sudden moisture change

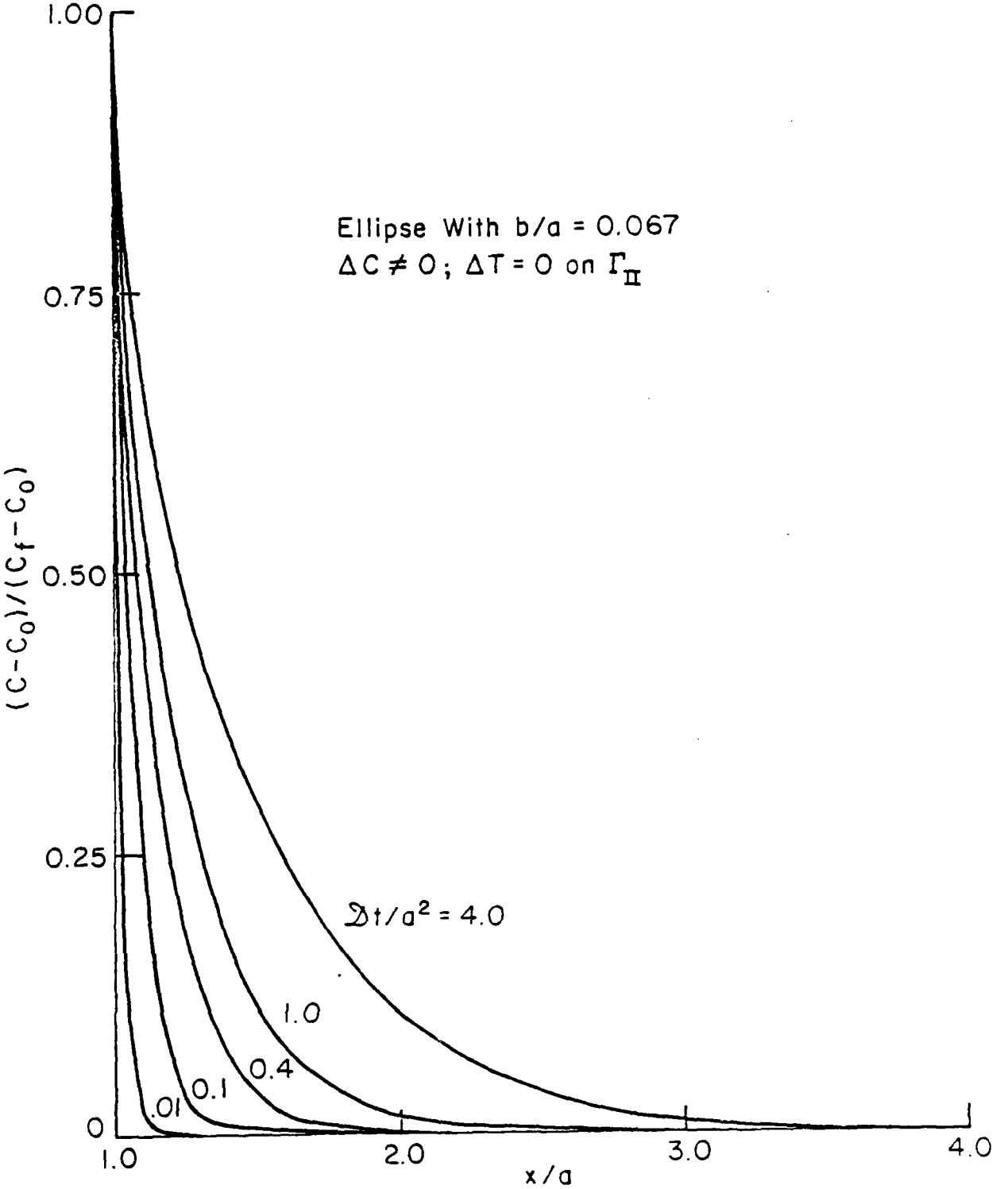

Figure 8 - Normalized moisture content versus distance for b/a = 0.067 and sudden moisture change

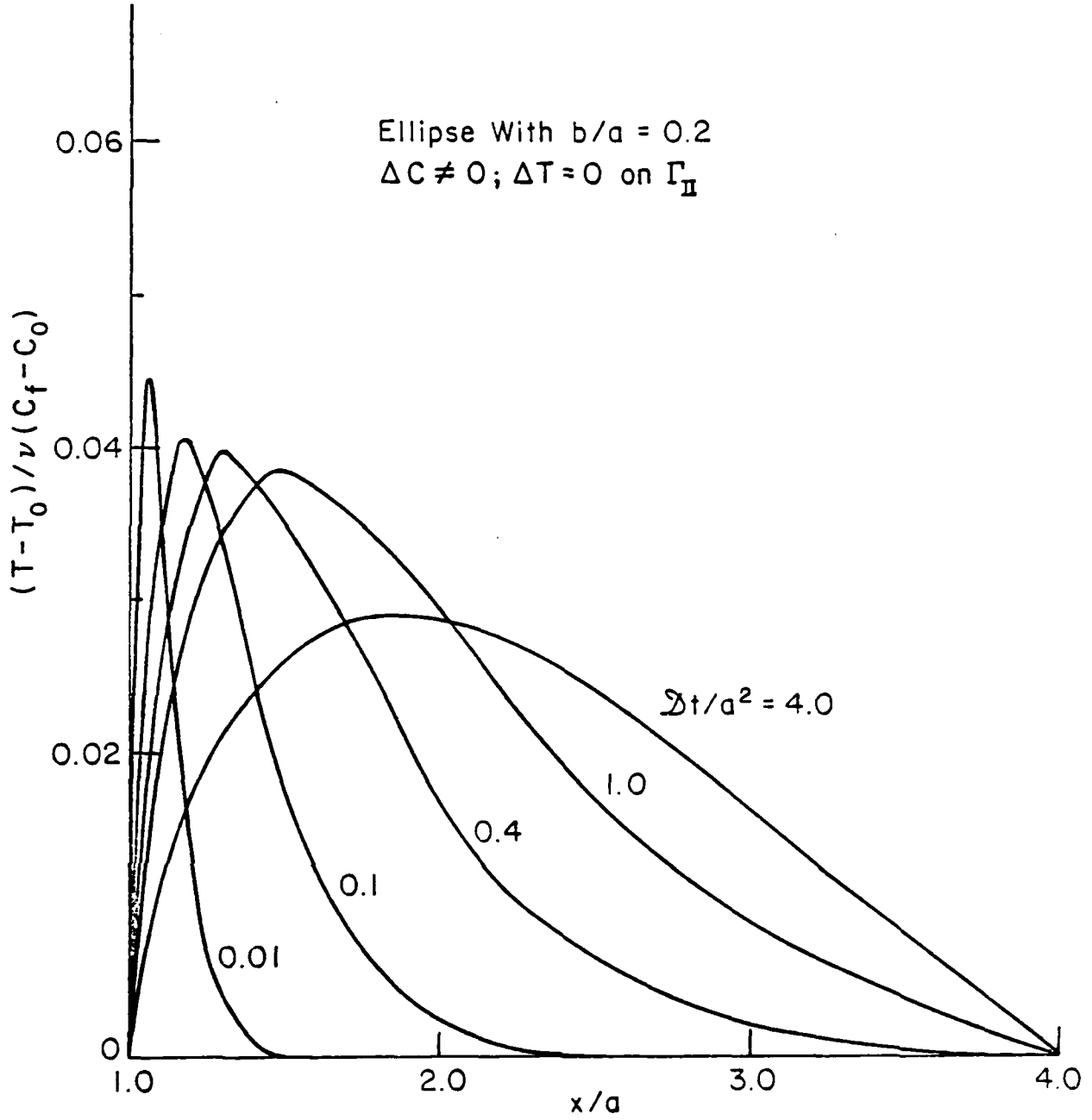

Figure 9 - Normalized temperature with distance for b/a = 0.2 and sudden moisture change

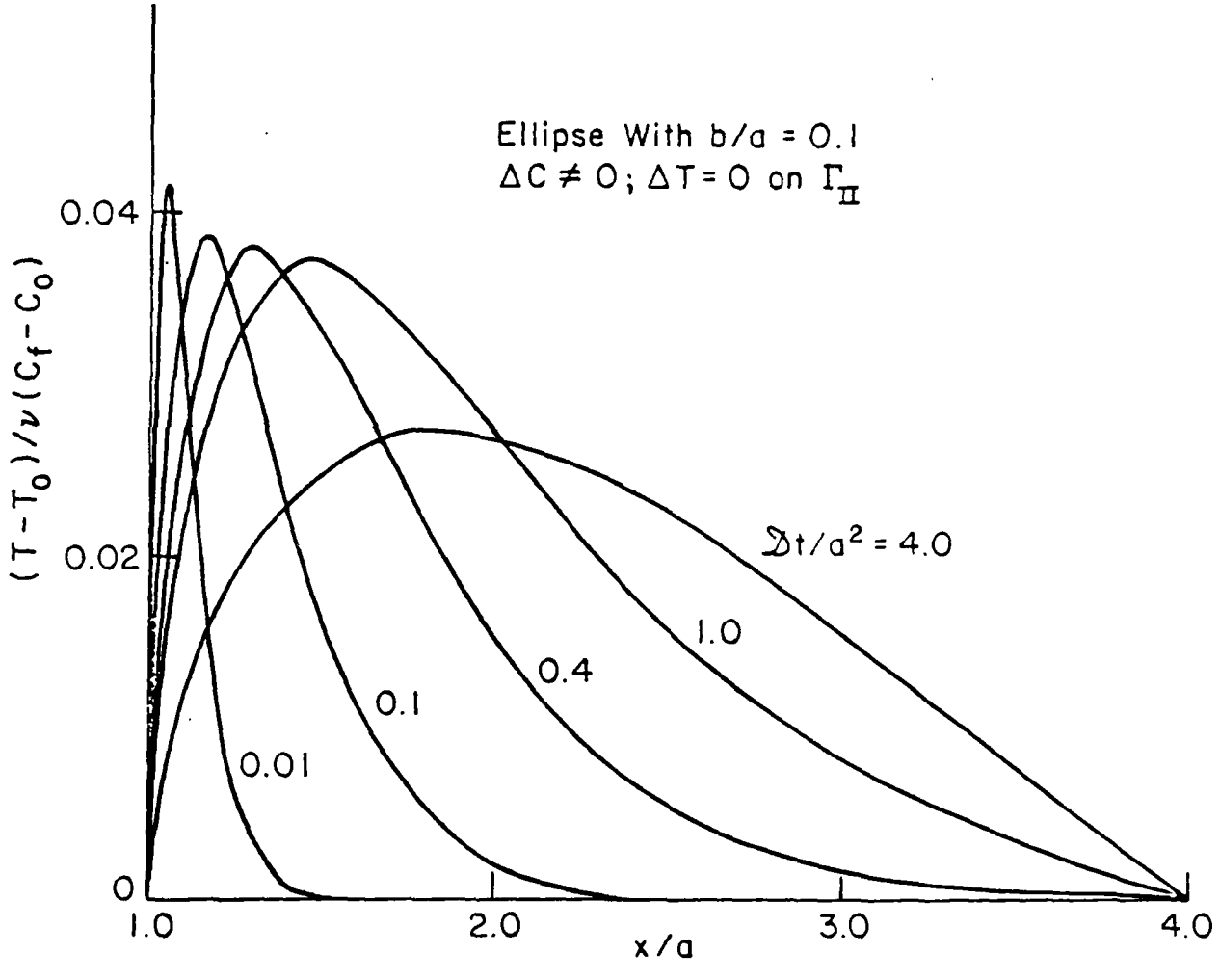

Figure 10 - Normalized temperature with distance for b/a = 0.1 and sudden moisture change

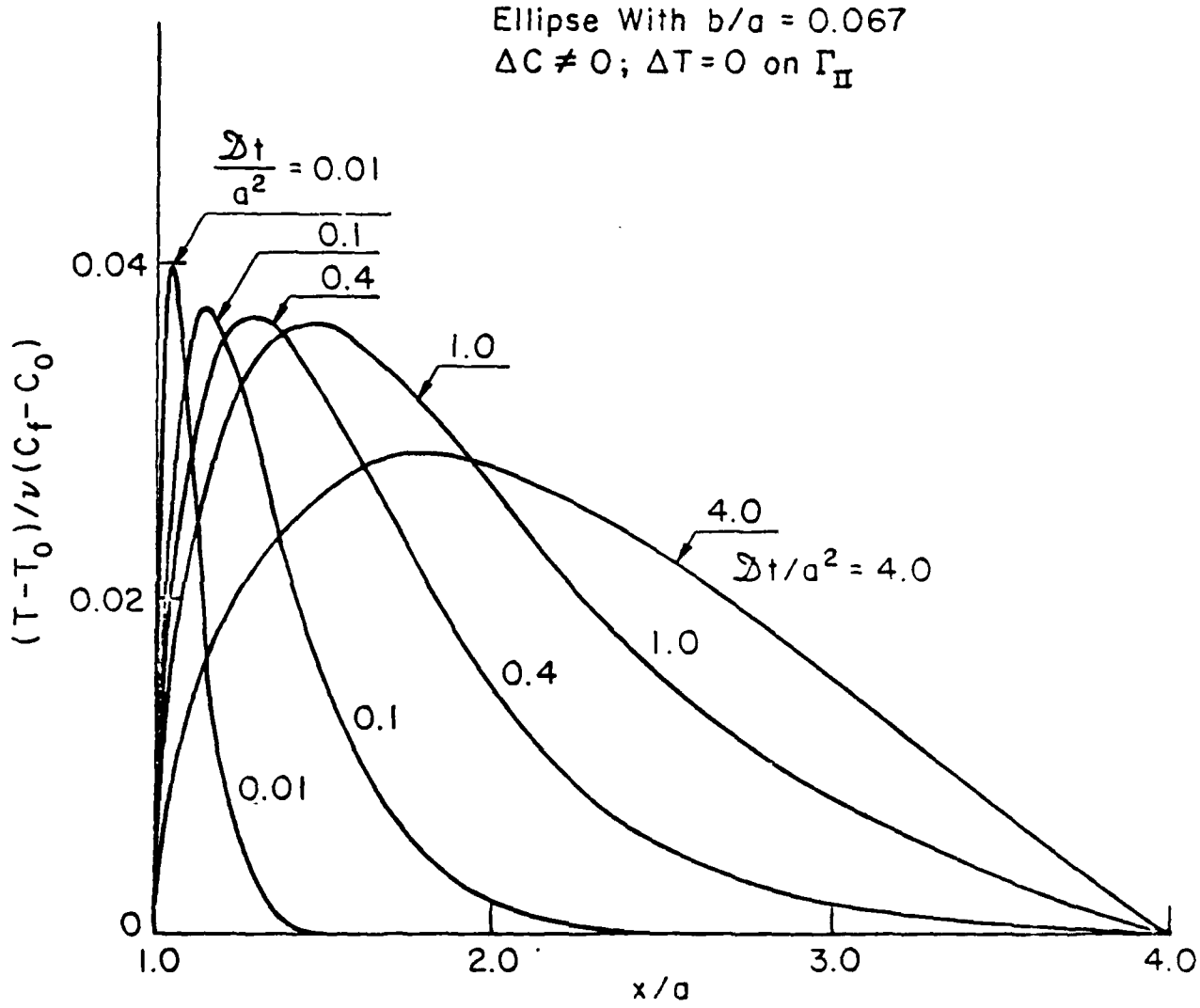

Figure 11 - Normalized temperature with distance for b/a = 0.067 and sudden moisture change

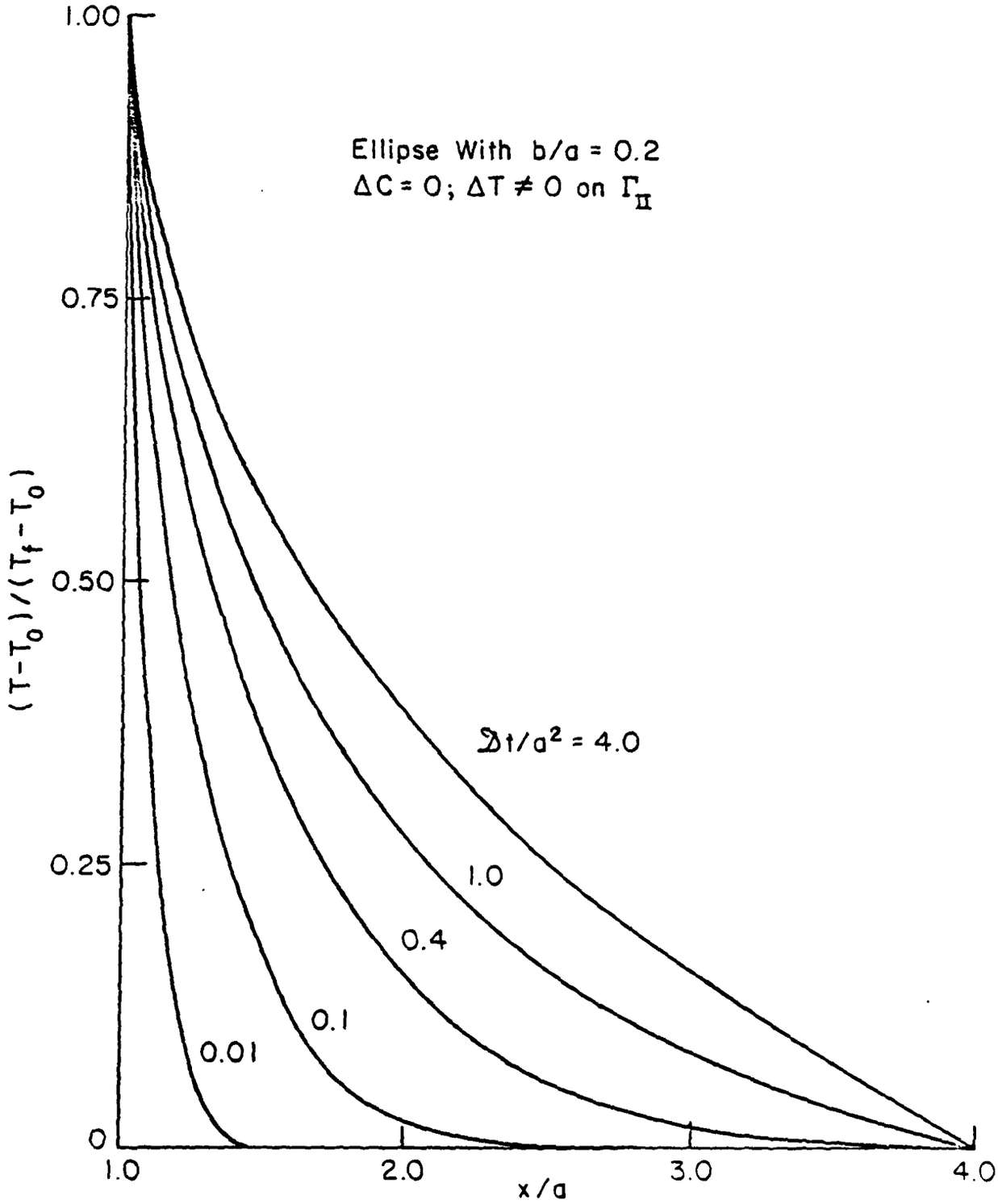

Figure 12 - Normalized temperature with distance for b/a = 0.2 and sudden temperature change

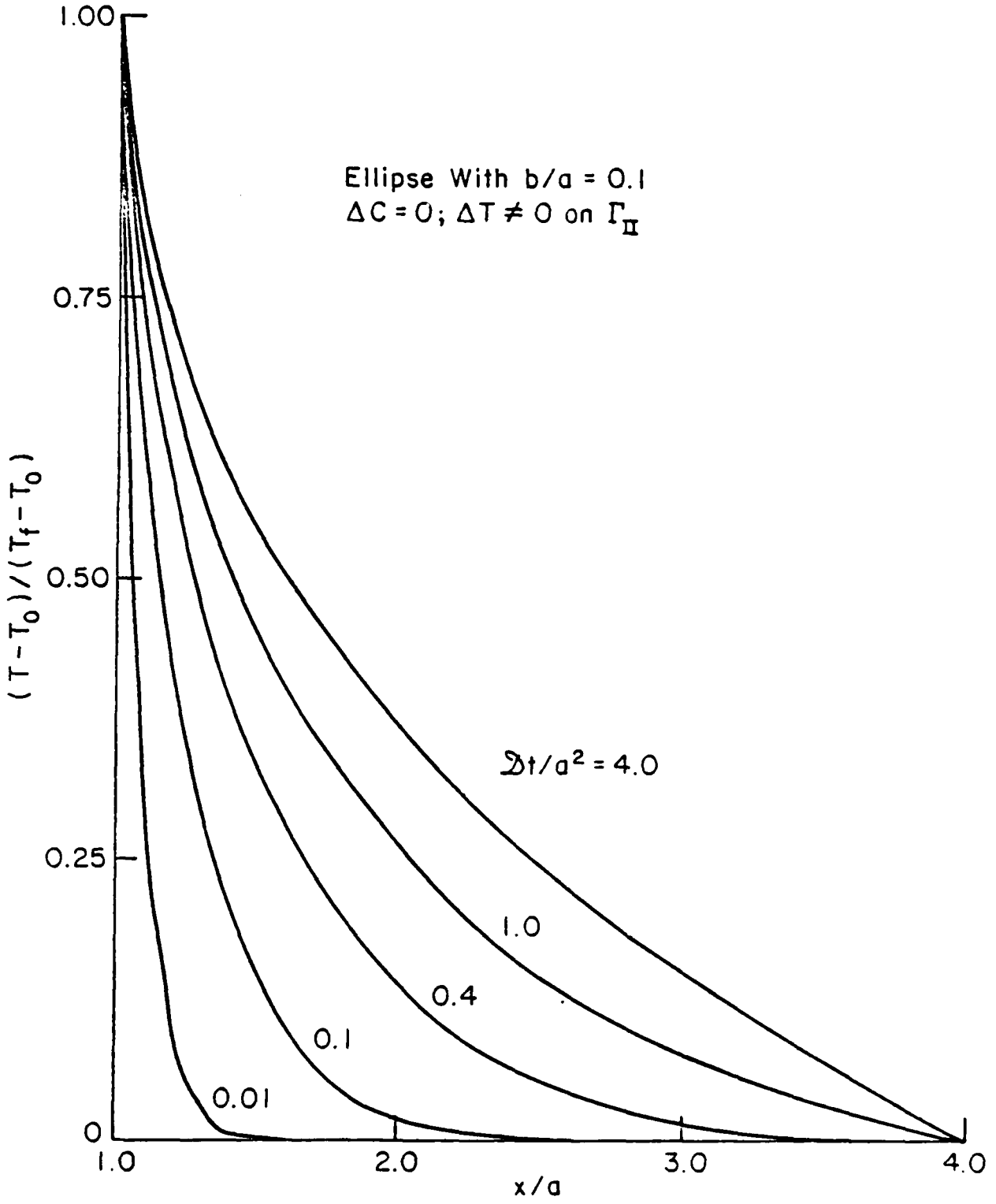

Figure 13 - Normalized temperature with distance for b/a = 0.1 and sudden temperature change

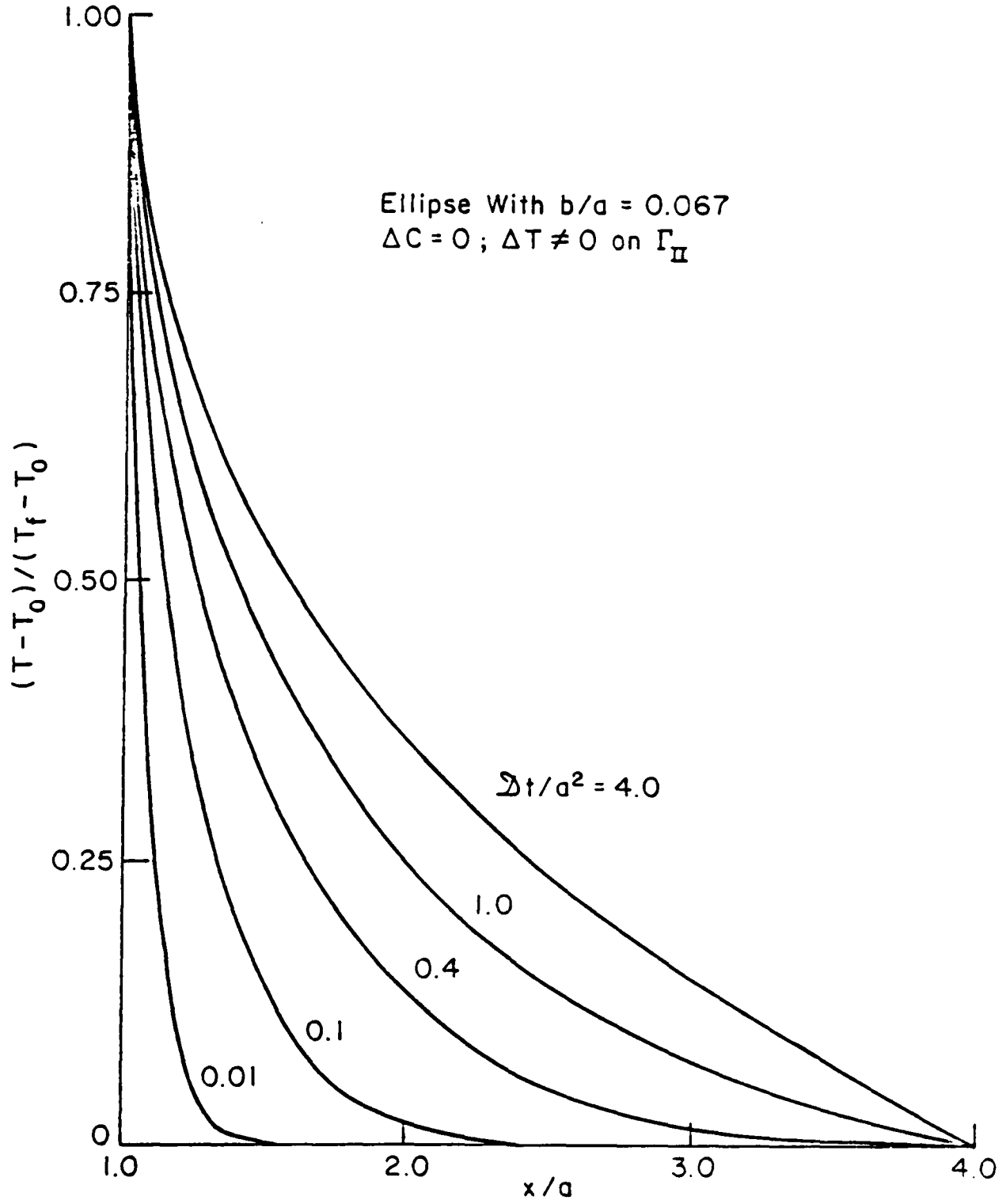

Figure 14 - Normalized temperature with distance for b/a = 0.067 and sudden temperature change

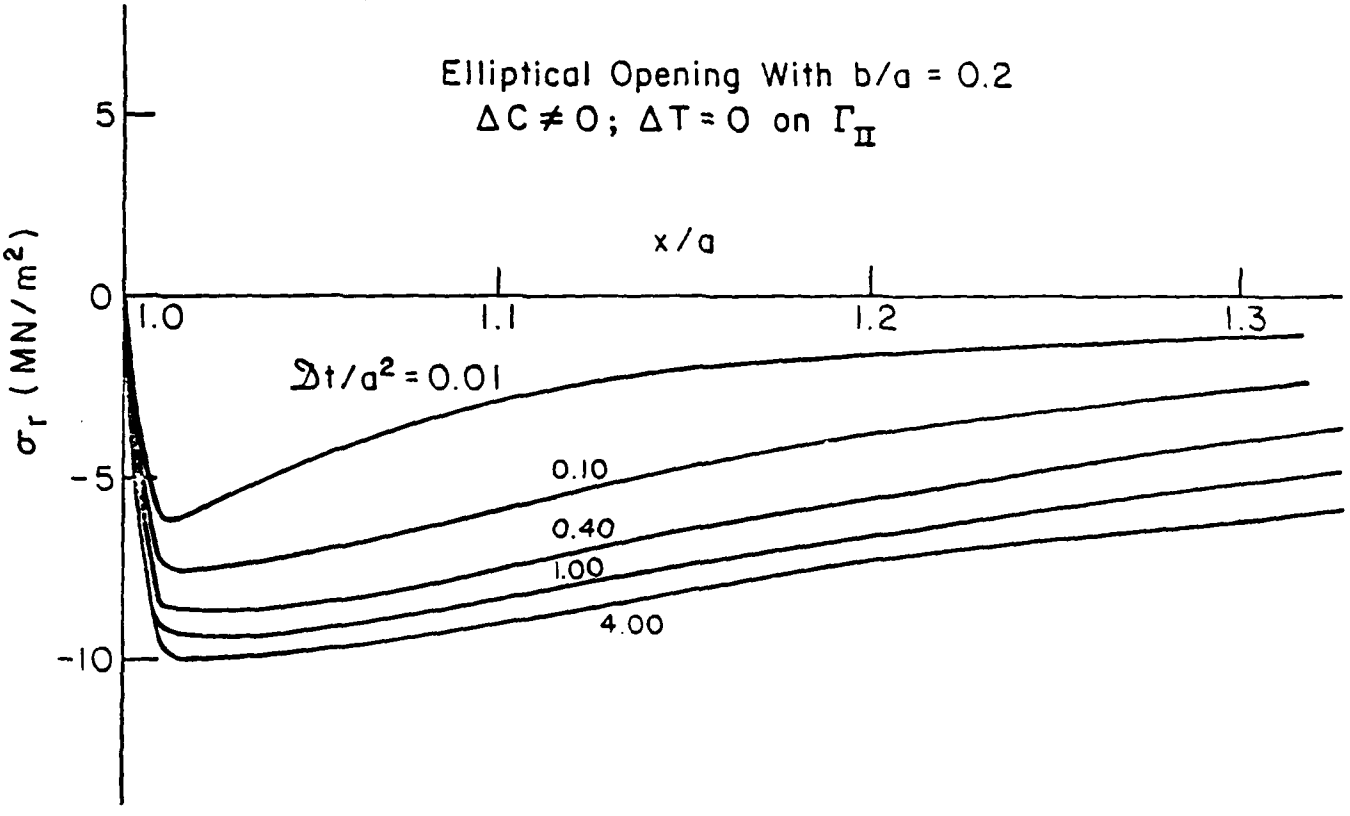

Figure 15 - Variations of radial stress with distance for b/a = 0.2 due to sudden moisture change

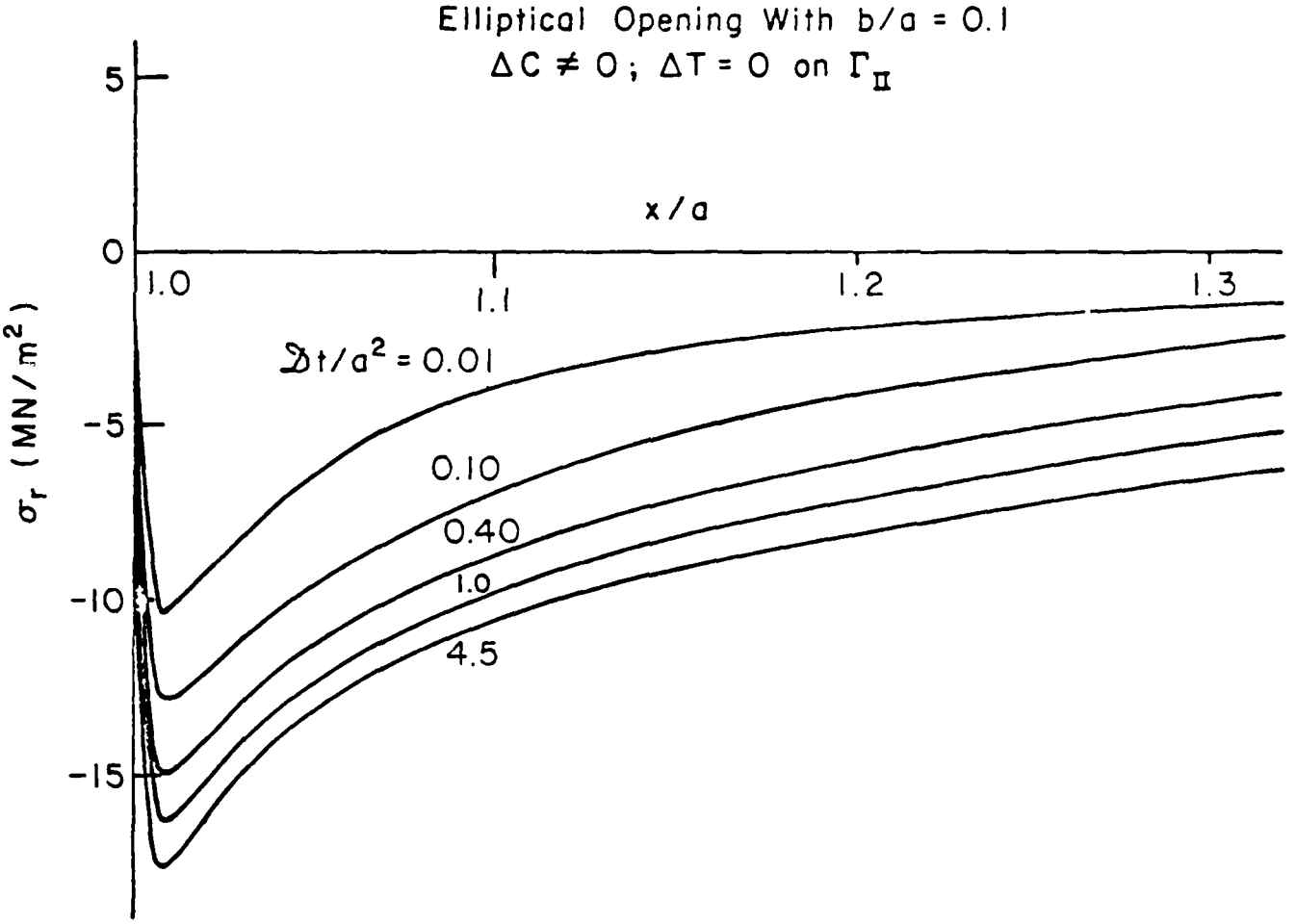

Figure 16 - Variations of radial stress with distance for b/a = 0.1 due to sudden moisture change

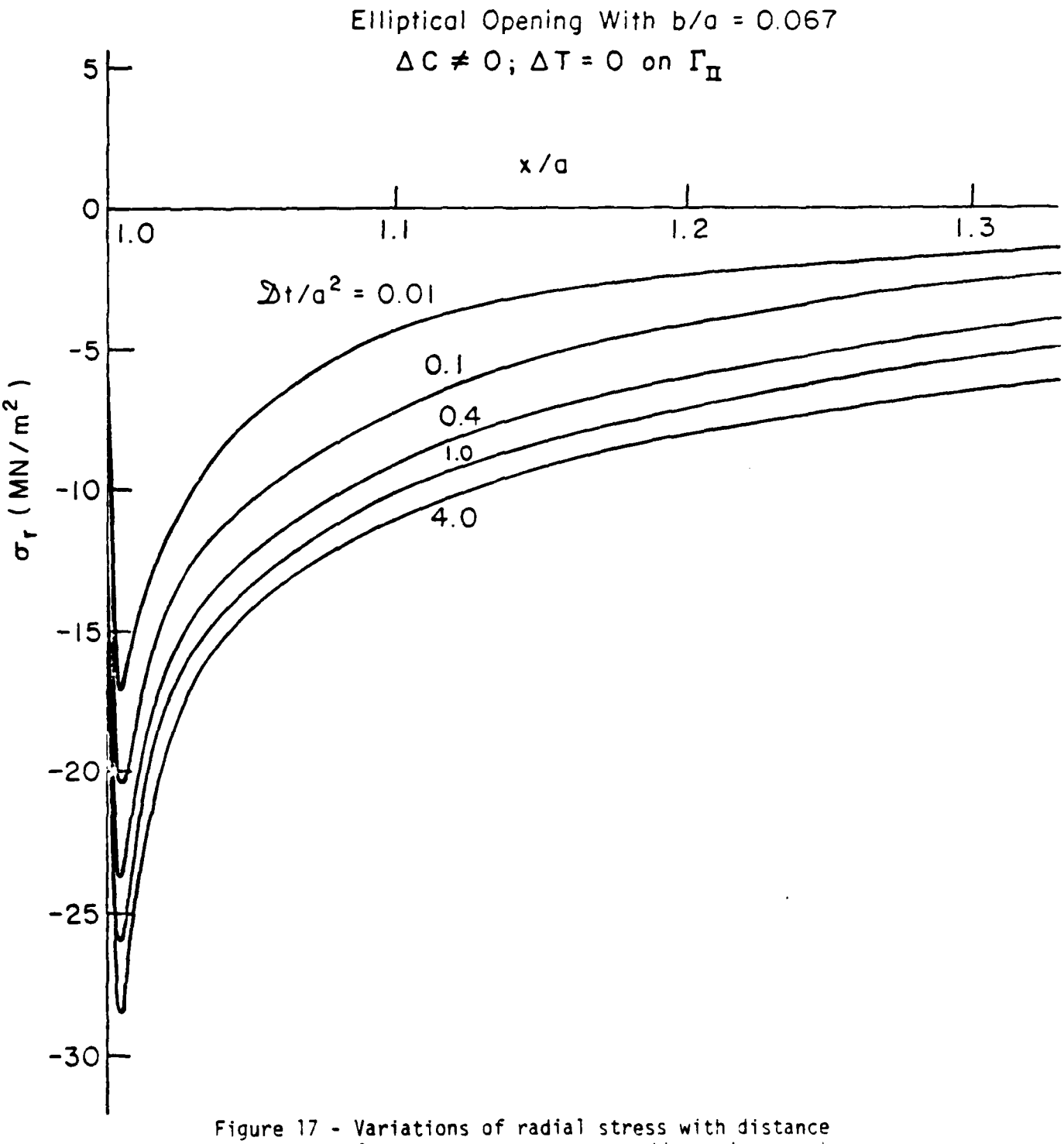

Figure 17 - Variations of radial stress with distance for b/a = 0.067 due to sudden moisture change

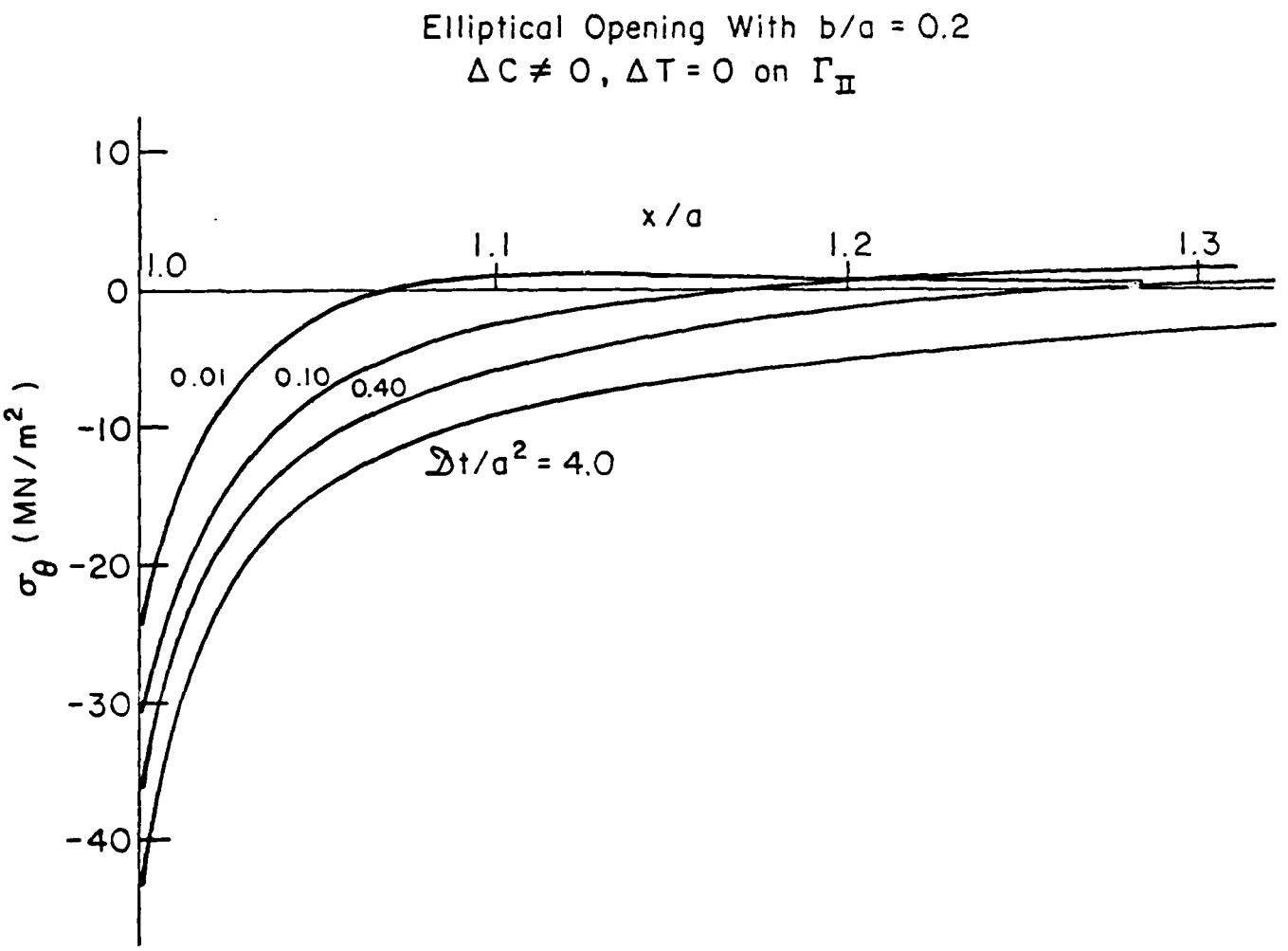

Figure 18 - Variations of circumferential stress with distance for b/a = 0.2 due to sudden moisture change

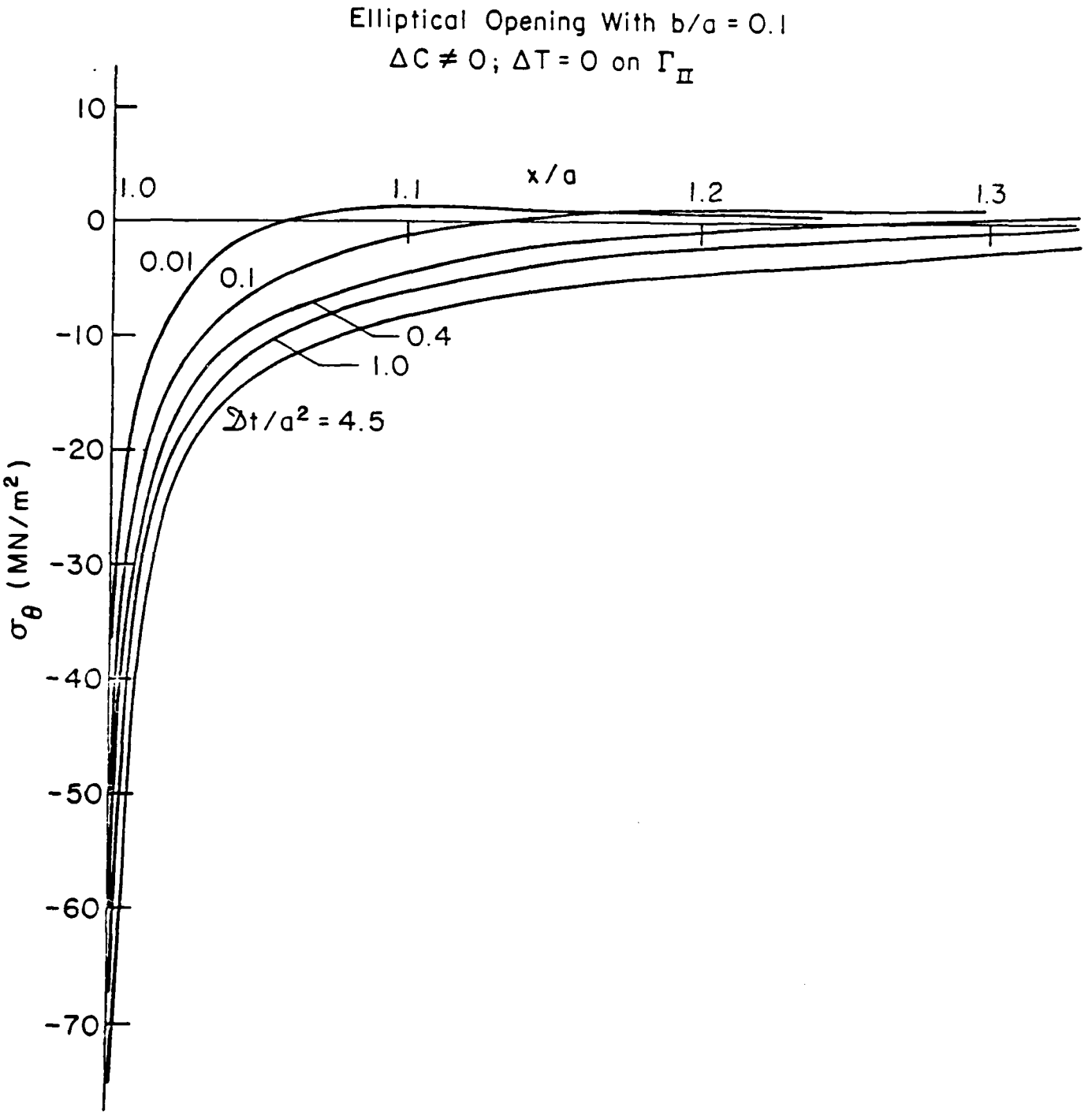

Figure 19 - Variations of circumferential stress with distance for b/a = 0.1 due to sudden moisture change

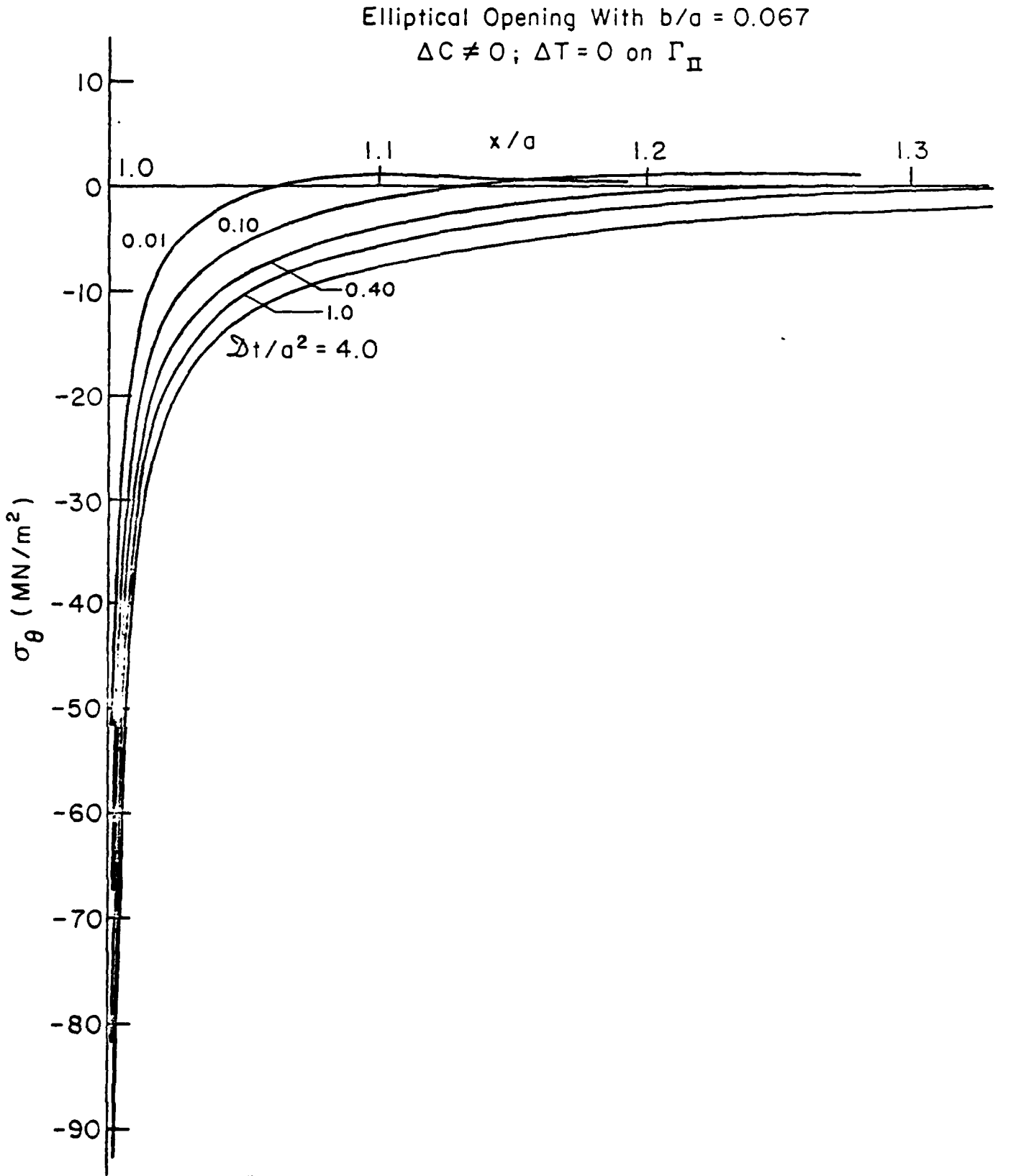

Figure 20 - Variations of circumferential stress with distance for b/a = 0.067 due to sudden moisture change

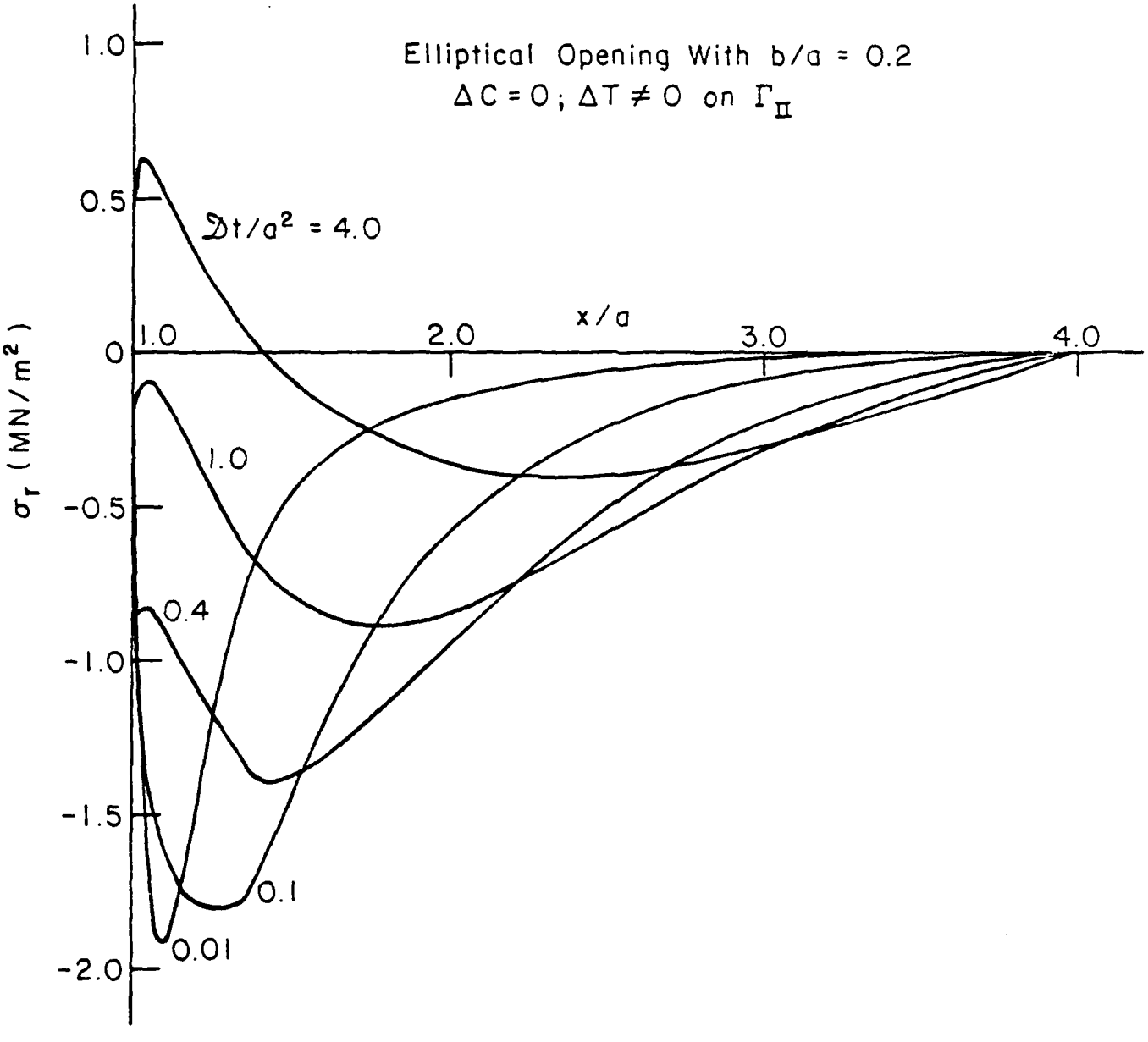

Figure 21 - Variations of radial stress with distance for b/a = 0.2 due to sudden temperature change

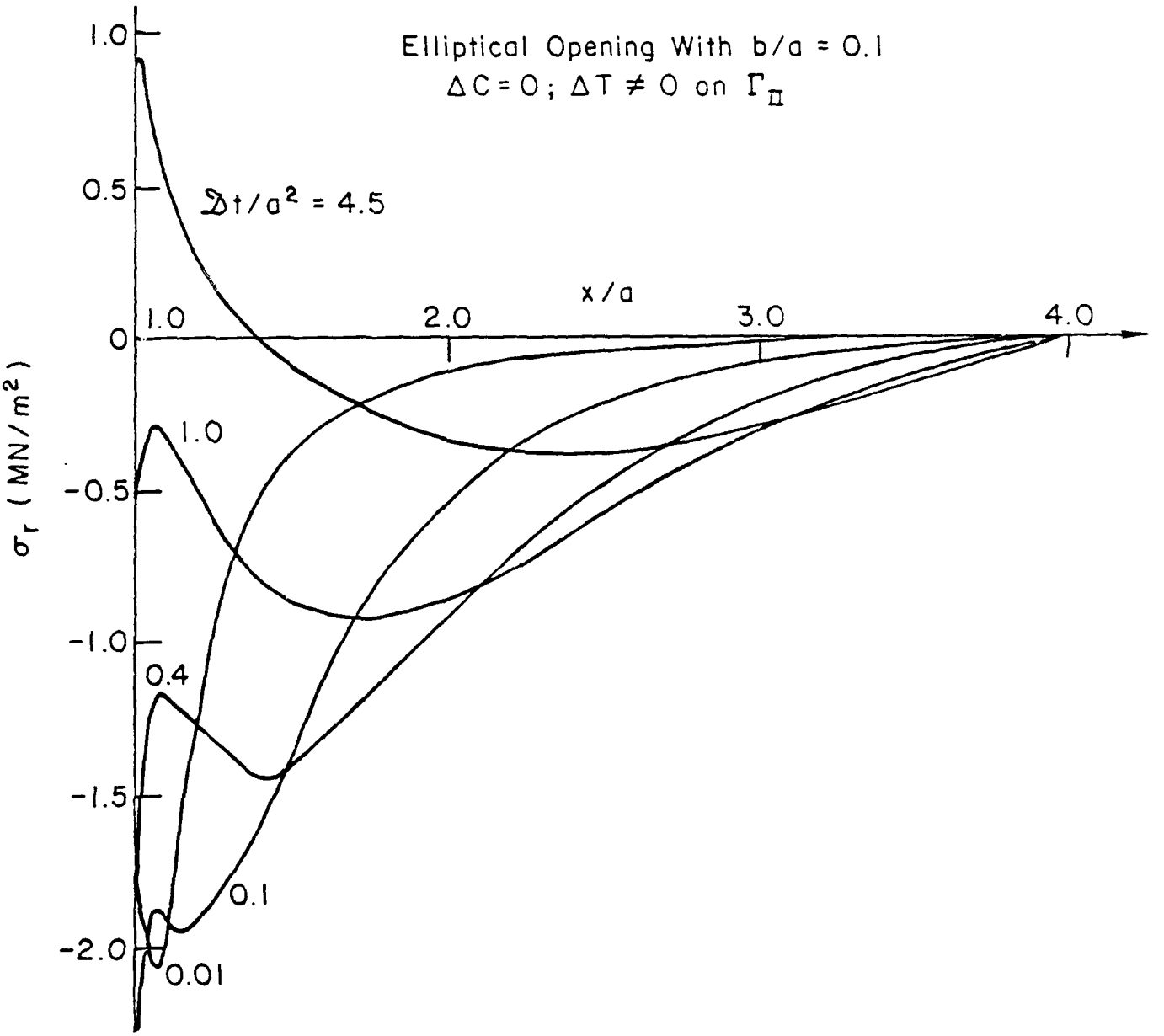

Figure 22 - Variations of radial stress with distance for b/a = 0.1 due to sudden temperature change

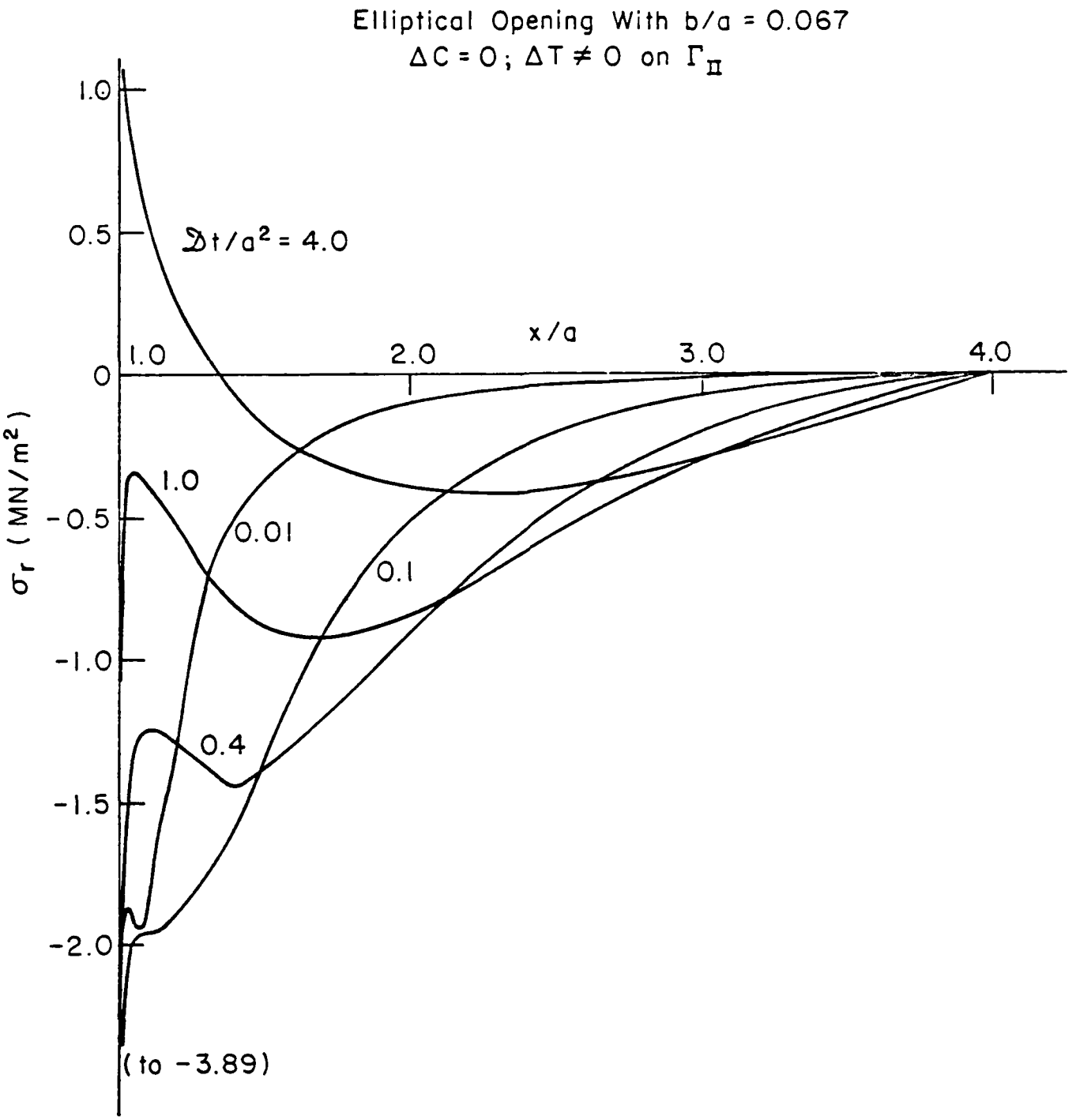

Figure 23 - Variations of radial stress with distance for b/a = 0.067 due to sudden temperature change

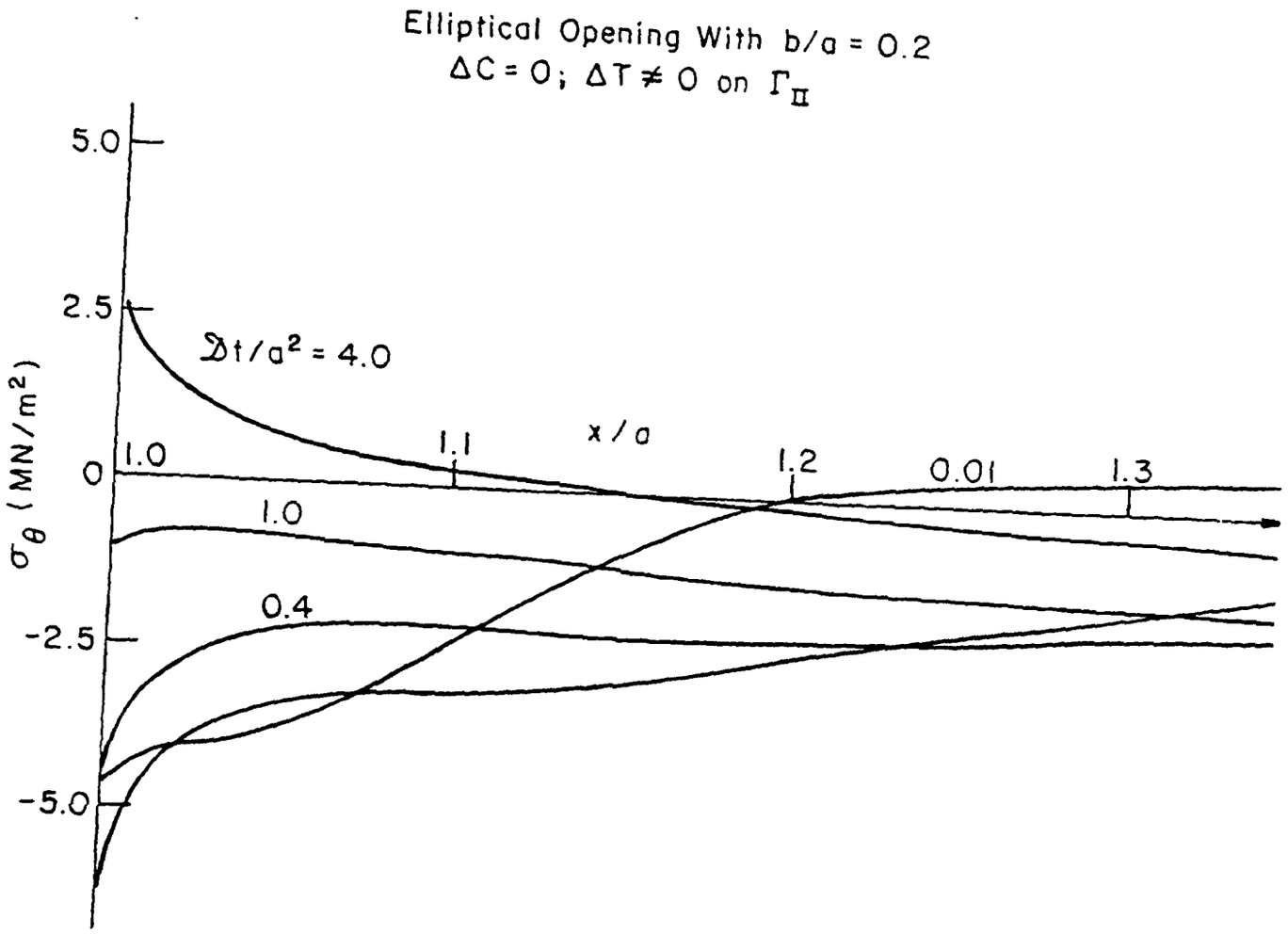

Figure 24 - Variations of circumferential stress with distance for b/a = 0.2 due to sudden temperature change

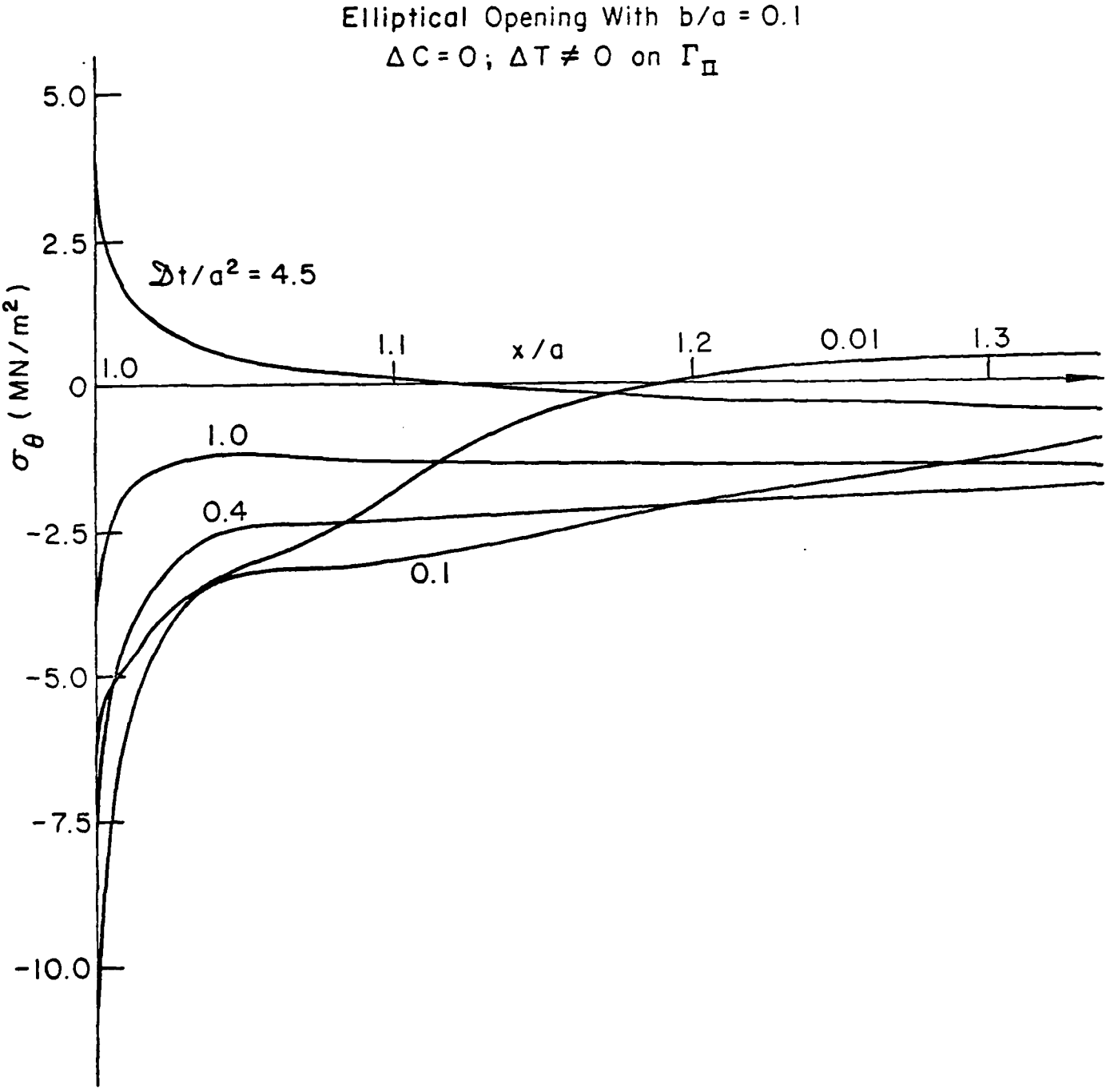

Figure 25 - Variations of circumferential stress with distance for b/a = 0.1 due to sudden temperature change

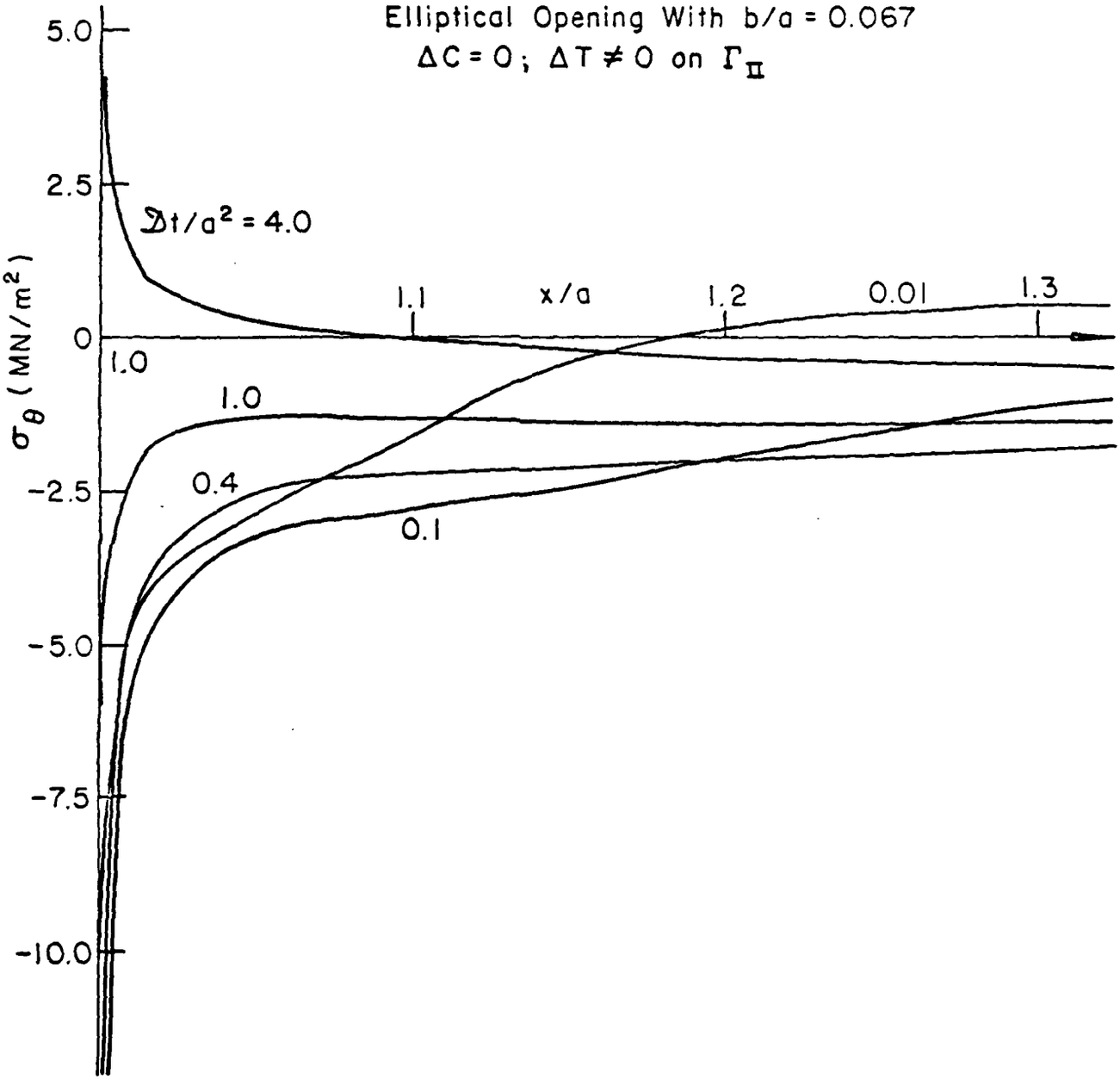

Figure 26 - Variations of circumferential stress with distance for b/a = 0.067 due to sudden temperature change

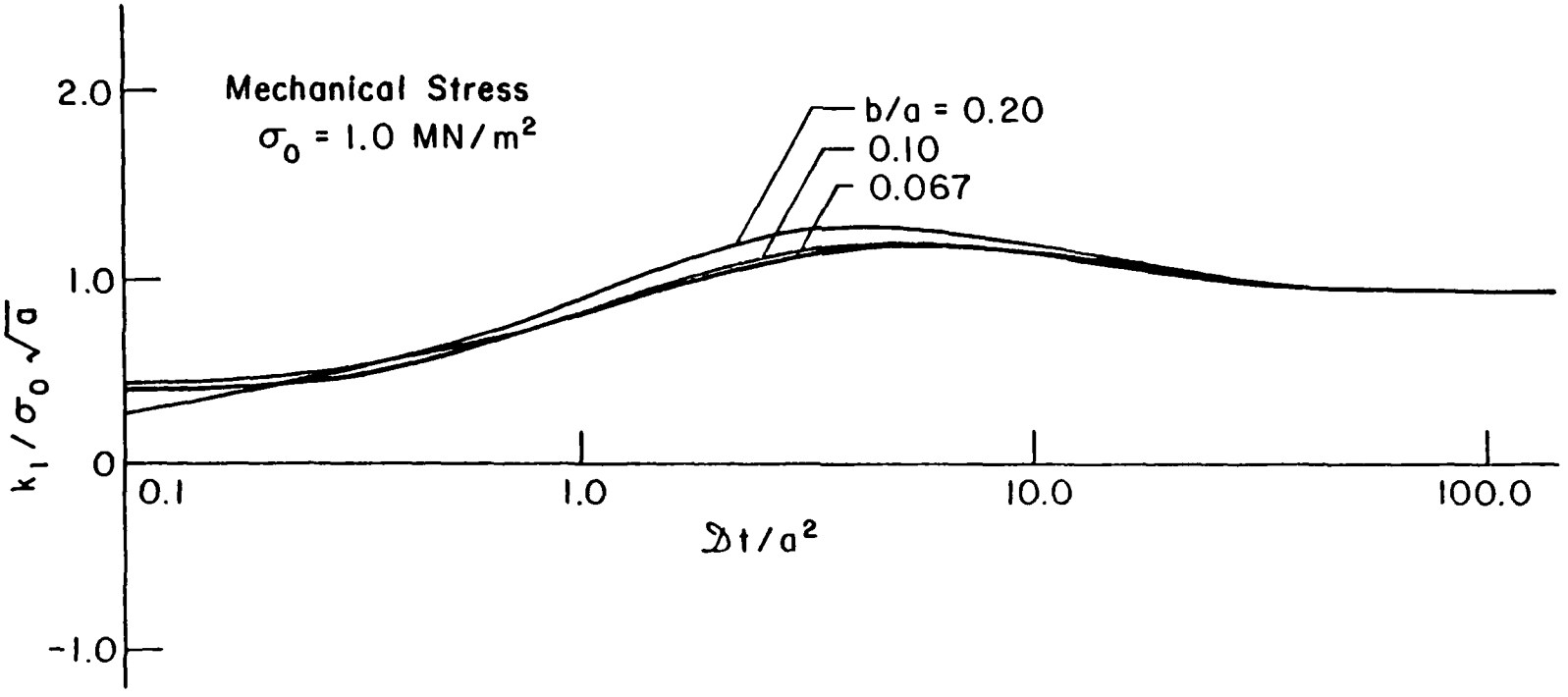

Figure 27 - Normalized stress intensity factor as a function of time for σ_0 = 1.0 MN/m^2

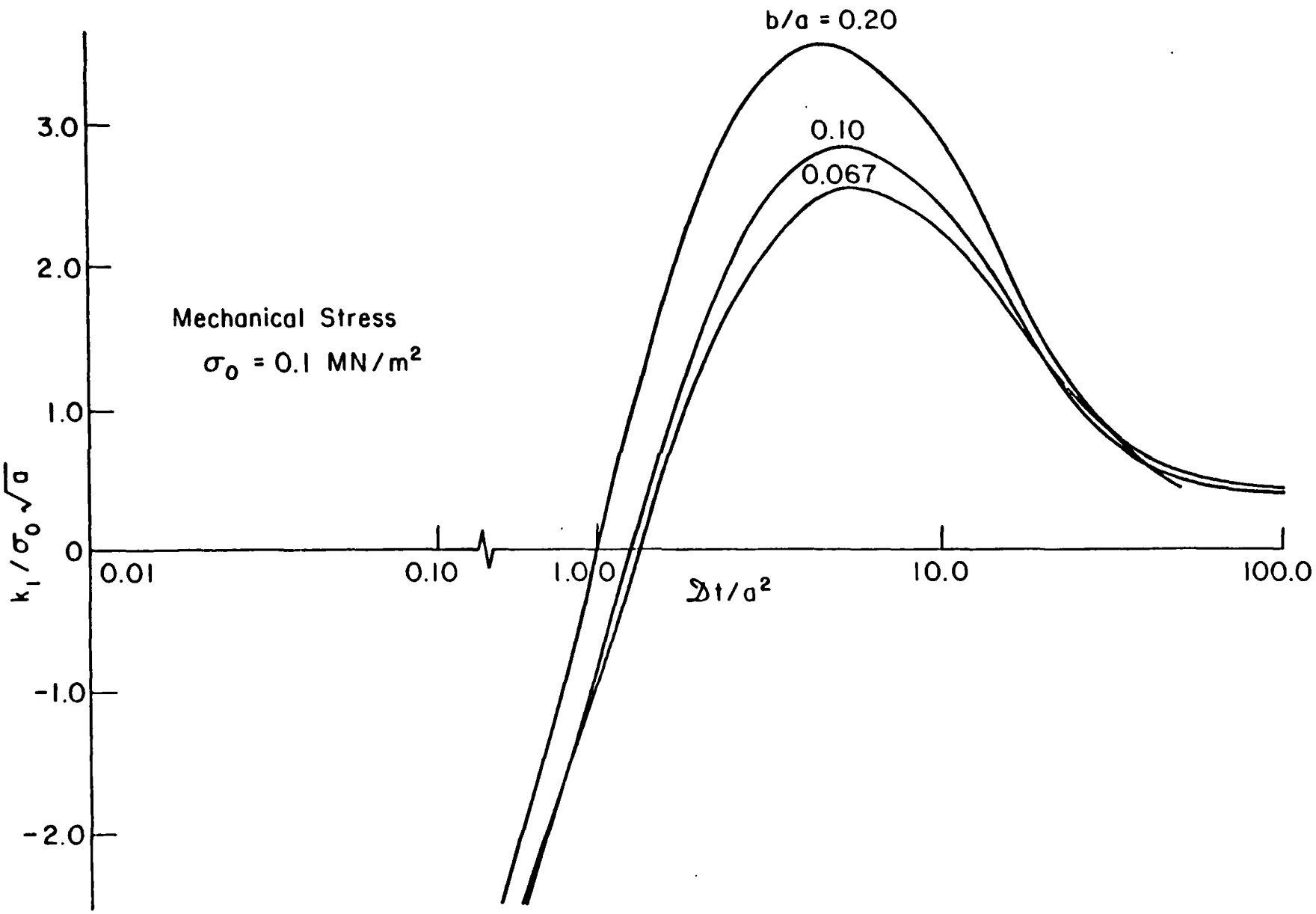

Figure 28 - Normalized stress intensity factor as a function of time for σ_0 = 0.1 MN/m^2

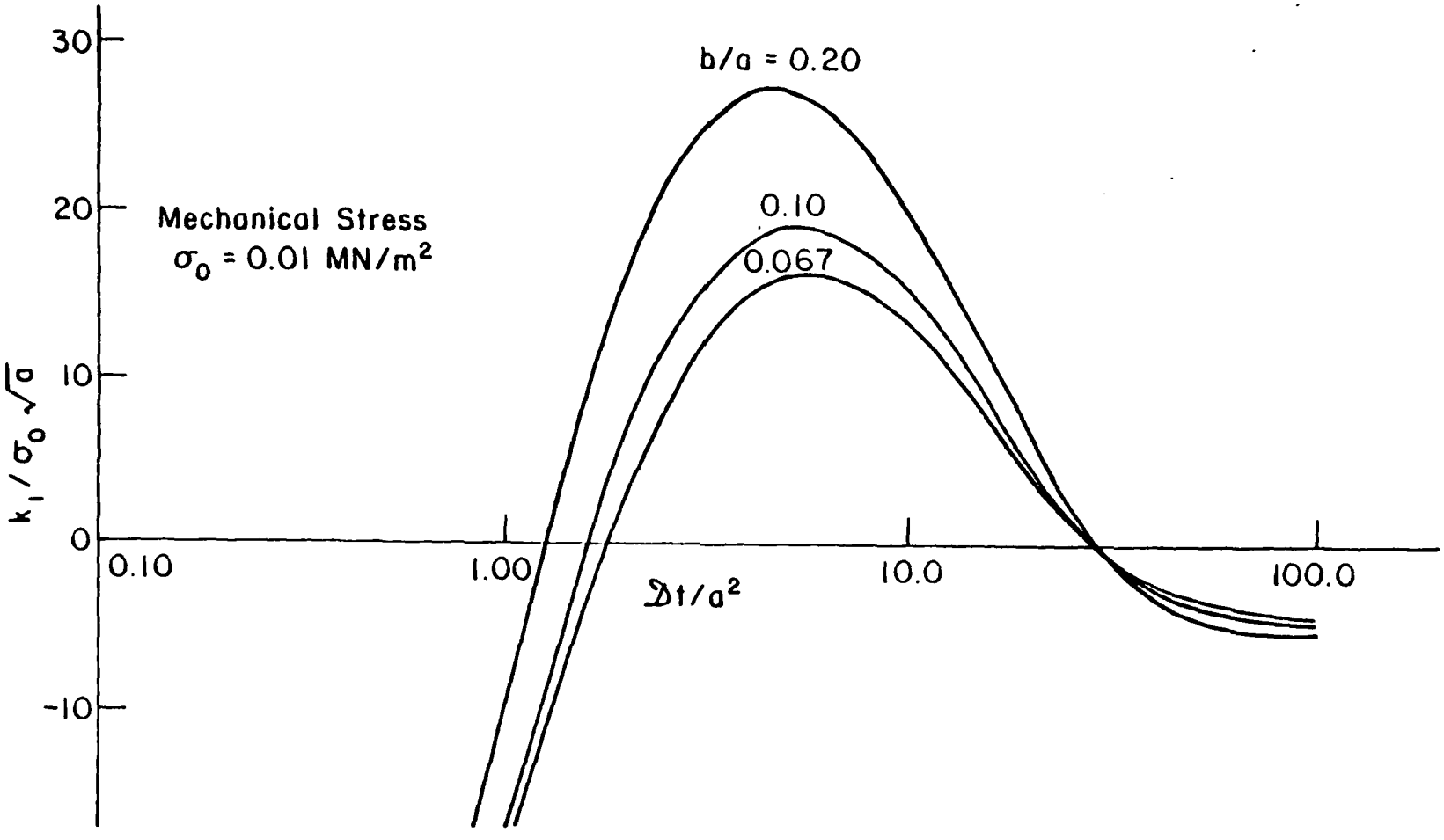

Figure 29 - Normalized stress intensity factor as a function of time for σ_0 = 0.01 MN/m^2

DISTRIBUTION LIST

	No. of Copies
Office of Deputy Under Secretary of Defense for Research and Engineering (ET) ATTN: Mr. J. Persh, Staff Specialist for Materials and Structures (Room 3D1089) The Pentagon Washington, DC 20301	1
Office of Deputy Chief of Research Development and Acquisition ATTN: DAMA-CSS/Dr. J. I. Bryant (Room 3D424) The Pentagon Washington, DC 20310	1
Commander U.S. Army Materiel Development and Readiness Command ATTN: DRCLDC, R. Gonano, Office of Laboratory Management 500 Eisenhower Avenue Alexandria, VA 22333	1
Director Ballistic Missile Defense Systems Command ATTN: BMDSC-TEN, Mr. N. J. Hurst	1
BMDSC-H	1
BMDSC-T	1
BMDSC-AOLIB P. O. Box 1500 Huntsville, AL 35807	1
Ballistic Missile Defense Program Office ATTN: DACS-BMT DARCOM Bldg., Seventh Floor 5001 Eisenhower Avenue Alexandria, VA 22333	1
Director Ballistic Missile Defense Advanced Technology Center ATTN: ATC-X, Dr. J. Carlson	1
ATC-X, Col. J. W. Gillespie	1
ATC-M, Mr. M. Whitfield	1
ATC-M, Dr. D. Harmon	1
ATC-M, Mr. J. Papadopoulos P. O. Box 1500 Huntsville, AL 35807	1

	No. of Copies
Director Defense Nuclear Agency ATTN: SPAS, Mr. D. Kohler Washington, DC 20305	1
Director Army Ballistic Research Laboratories ATTN: DRDAR-BLT, Dr. N. J. Huffington, Jr. DRDAR-BLT, Dr. T. W. Wright DRDAR-BLT, Dr. G. L. Moss Aberdeen Proving Ground, MD 21005	1 1 1
Commander Harry Diamond Laboratories ATTN: DRXDO-NP, Dr. F. Wimenitz 2800 Powder Mill Road Adelphi, MD 20783	1
Commander U.S. Army Combat Development Command Institute of Nuclear Studies ATTN: Technical Library Fort Bliss, TX 79916	1
Commander Air Force Materials Laboratory Air Force Systems Command ATTN: LNE/Dr. W. Kessler LNC/Dr. D. Schmidt Wright-Patterson Air Force Base, OH 45433	1 1
Commander BMO/ABES Office ATTN: BMO/MNRT, Col. R. Smith BMO/MNRTE, Maj. J. Sikra BMO/MNRTE, Maj. K. Yelmgren Norton Air Force Base, CA 92409	1 1 1
Commander Air Force Materials Laboratory ATTN: AFML/MBM, Dr. S. W. Tsai Wright-Patterson Air Force Base, OH 45433	1

	No. of Copies
Commander Naval Ordnance Systems Command ATTN: ORD-03331, Mr. M. Kinna Washington, DC 20360	1
Commander Naval Surface Weapons Center ATTN: Dr. C. Lyons Dr. W. Messick Silver Springs, MD 20910	1 1
Lawrence Livermore Laboratory ATTN: Dr. E. M. Wu P. O. Box 808 (L-342) Livermore, CA 94550	1
Los Alamos Scientific Laboratory ATTN: GMX-6, Dr. J. W. Taylor P. O. Box 1663 Los Alamos, NM 87544	1
Sandia Laboratories ATTN: Dr. Frank P. Gerstle, Jr. Dr. L. D. Bertholf Dr. J. Lipkin P. O. Box 5800 Albuquerque, NM 87115	1 1 1
Aerospace Corporation ATTN: Dr. R. Cooper P. O. Box 92957 Los Angeles, CA 90009	1
AVCO Corporation Government Products Group ATTN: Dr. W. Reinecke Mr. P. Rolincik 201 Lowell Street Wilmington, MA 01997	1 1
ETA Corporation ATTN: Mr. D. L. Mykkanen P. O. Box 6625 Orange, CA 92667	1

	No. of Copies
Effects Technology, Inc.	
ATTN: Dr. R. Wengler	1
Dr. R. Parisse	1
Mr. J. Green	1
5383 Hollister Avenue	
Santa Barbara, CA 93111	
Fiber Materials, Inc.	
ATTN: Mr. M. Subilia, Jr.	1
Mr. L. Landers	1
Mr. G. Williams	1
Mr. P. Marchol	1
Biddeford Industrial Park	
Biddeford, ME 04005	
General Electric Company	
Advanced Materials Development Laboratory	
ATTN: Mr. K. Hall	1
Mr. J. Brazel, Room 4466	1
Ms. B. McGuire	1
Mr. L. Gilbert	1
3198 Chestnut Street	
Philadelphia, PA 19101	
General Dynamics Corporation	
Convair Division	
ATTN: Mr. J. Hertz	1
Mr. H. McCutcheon, Jr.	1
5001 Kearny Villa Road	
San Diego, CA 92138	
General Dynamics Corporation	
ATTN: Dr. D. J. Wilkins, Mail Zone 2884	1
P. O. Box 748	
Fort Worth, TX 76101	
Kaman Sciences Corporation	
ATTN: Mr. F. Shelton	1
P. O. Box 7463	
Colorado Springs, CO 80933	
Ktech	
ATTN: Dr. D. Keller	1
911 Pennsylvania Avenue, N.E.	
Albuquerque, NM 87110	

	No. of Copies
Lockheed Missiles and Space Company ATTN: Mr. D. Aspinwall P. O. Box 504 Sunnyvale, CA 94088	1
Martin Marietta Aerospace ATTN: Mr. V. Hewitt Mr. Frank H. Koo P. O. Box 5837 Orlando, FL 32805	1 1
McDonnell Douglas Corporation ATTN: Dr. L. Cohen Mr. H. Parachanian 5301 Bolsa Avenue Huntington Beach, CA 92647	1 1
Prototype Development Associates, Inc. ATTN: Mr. J. Schultzler Mr. N. Harrington 1740 Garry Avenue, Suite 201 Santa Ana, CA 92705	1 1
R&D Associates ATTN: Dr. A. Field 525 Wilshire Blvd. Santa Monica, CA 90025	1
Radkowski Associates ATTN: Dr. P. Radkowski P. O. Box 5474 Riverside, CA 92507	1
Southwest Research Institute ATTN: Mr. A. Wenzel 8500 Culebra Road San Antonio, TX 78206	1
Stanford Research Institute ATTN: Dr. D. Curran Dr. L. Seaman 333 Ravenswood Avenue Menlo Park, CA 90250	1 1

	No. of Copies
Terra Tek, Inc. ATTN: Dr. A. H. Jones 420 Wakara Way Salt Lake City, Utah 84108	1
TRW Systems Group ATTN: Mr. D. Gamble One Space Park Redondo Beach, CA 90278	1
Stanford University Department of Applied Mechanics ATTN: Professor E. H. Lee Stanford, CA 94305	1
University of Illinois at Chicago Circle Department of Materials Engineering ATTN: Professor R. L. Spilker Professor T. C. T. Ting Chicago, IL 60680	1 1
Defense Documentation Center Cameron Station, Bldg. 5 5010 Duke Station Alexandria, VA 22314	1
Director Army Materials & Mechanics Research Center ATTN: DRXMR-H, Mr. J. F. Dignam DRXMR-H, Dr. S. C. Chou DRXMR-H, Mr. L. R. Aronin DRXMR-H, Dr. D. P. Dandekar DRXMR-AP DRXMR-PL DRXMR-PR Watertown, MA 02172	 1 1 1 1 1 2 1

Army Materials and Mechanics Research Center
Watertown, Massachusetts 02172

AD
UNCLASSIFIED

TRANSIENT HYGROTHERMAL AND MECHANICAL STRESS INTENSITIES AROUND ELLIPTICAL CAVITIES

UNLIMITED DISTRIBUTION

G. C. Sih and A. Ogawa
Lehigh University, Bethlehem, Pennsylvania 18015

Key Words

Final Report AMMRC TR 80-32, August 1980, 54 pp
Illus - Tables, Contract DAAG46-79-C-0049

Hygrothermal effect
Moisture content
Temperature
Finite element
Transient response
Composite
Crack
Stress intensities

The transient hygrothermal stresses are determined by assuming that heat and moisture are coupled. A system of coupled diffusion equations is solved by a finite element scheme allowing for time dependent changes in the moisture and/or temperature on the surfaces of the T300/5208 epoxy resin for the graphite/epoxy fiber reinforced composite. The time dependent portion of the problem was solved by means of Laplace transformation. Particular emphases are given to the evaluation of transient stresses around a mechanical imperfection in the form of a narrow ellipse. Numerical results are displayed graphically for three different values of the semi-minor to semi major axis ratio.
A stress intensity factor parameter commonly used in fracture mechanics is defined for a narrow ellipse and calculated to investigate the influence of stresses induced by hygrothermal and mechanical disturbances. The radius of curvature of the elliptical cavity can significantly affect the combined stress intensity near the cavity ends. The maximum stress intensities occur at different times depending on the cavity geometry and proportion of the hygrothermal and mechanical loading. These results could shed light on composite failure under conditions where heat and moisture play a role.

Army Materials and Mechanics Research Center
Watertown, Massachusetts 02172

AD
UNCLASSIFIED

TRANSIENT HYGROTHERMAL AND MECHANICAL STRESS INTENSITIES AROUND ELLIPTICAL CAVITIES

UNLIMITED DISTRIBUTION

G. C. Sih and A. Ogawa
Lehigh University, Bethlehem, Pennsylvania 18015

Key Words

Final Report AMMRC TR 80-32, August 1980, 54 pp
Illus - Tables, Contract DAAG46-79-C-0049

Hygrothermal effect
Moisture content
Temperature
Finite element
Transient response
Composite
Crack
Stress intensities

The transient hygrothermal stresses are determined by assuming that heat and moisture are coupled. A system of coupled diffusion equations is solved by a finite element scheme allowing for time dependent changes in the moisture and/or temperature on the surfaces of the T300/5208 epoxy resin for the graphite/epoxy fiber reinforced composite. The time dependent portion of the problem was solved by means of Laplace transformation. Particular emphases are given to the evaluation of transient stresses around a mechanical imperfection in the form of a narrow ellipse. Numerical results are displayed graphically for three different values of the semi-minor to semi major axis ratio.
A stress intensity factor parameter commonly used in fracture mechanics is defined for a narrow ellipse and calculated to investigate the influence of stresses induced by hygrothermal and mechanical disturbances. The radius of curvature of the elliptical cavity can significantly affect the combined stress intensity near the cavity ends. The maximum stress intensities occur at different times depending on the cavity geometry and proportion of the hygrothermal and mechanical loading. These results could shed light on composite failure under conditions where heat and moisture play a role.